Turkish Journal of Earth Sciences (Turkish J. Earth Sci.), Vol. 19, 2010, pp. 123–156. Copyright ©TÜBİTAK
doi:10.3906/yer-0904-1 First published online 30 April 2009

Testing Miocene Remagnetization of Bey Dağları: Timing and Amount of Neogene Rotations in SW Turkey

DOUWE J.J. VAN HINSBERGEN[1,2], MARK J. DEKKERS[1] & AYTEN KOÇ[1,3]

[1] Palaeomagnetic Laboratory 'Fort Hoofddijk', Faculty of Geosciences, Utrecht University,
Budapestlaan 17, 3584 CD Utrecht, The Netherlands
(E-mail: douwework@gmail.com)

[2] Now at: Center for Geodynamics, Physics of Geological Processes, University of Oslo,
Sem Sælands vei 24, 0316 Oslo, Norway

[3] Middle East Technical University, Department of Geological Engineering, TR–06531 Ankara, Turkey

Received 07 December 2009; revised typescript receipt 07 December 2009; accepted 07 December 2007

Abstract: Here we reassess the timing and amount of rotation of the eastern limb of the Aegean orocline, located in SW Turkey. The current model for this orocline involves a 25–30° counterclockwise (CCW) rotation of the Bey Dağları region, which exposes upper Cretaceous to Eocene platform carbonates and lower Miocene flysch deposits. In this model the rotation has to postdate a Miocene remagnetization, which would not exclude non-synchroneity between rotations of the western and eastern limbs of the Aegean orocline. To test this model a detailed palaeomagnetic study was conducted on lower Miocene strata in the Bey Dağları area. Two (composite) sections were sampled near Korkuteli and Doğantaş, spanning the lower Miocene foreland basin stratigraphy from the Aquitanian unconformity with the Bey Dağları limestones to the uppermost Burdigalian–lowermost Langhian, and a wide array of palaeomagnetic analyses were obtained.

The natural remanent magnetization (NRM) in the Aquitanian limestones and Burdigalian blue clays resides dominantly in magnetite with minor greigite and haematite. A positive reversals test, a correlation of obtained polarity patterns to the geomagnetic polarity timescale, showing significant compaction following acquisition of the NRM, a scatter in NRM directions that can be confidently attributed to palaeosecular variation and a positive recently-proposed end-member model test of the acquisition curves of isothermal remanent magnetization (IRM) all show that the Miocene sediments on the Bey Dağları platform have not been remagnetized.

Our new results, combined with a partial reassessment of existing data, imply that the Bey Dağları region underwent no rotation between the late Cretaceous and late Burdigalian, and 20° counterclockwise rotation between 16 and 5 Ma, i.e. during the middle to late Miocene and prior to deposition of previously reported non-rotated Pliocene sediments north of Antalya. The two limbs of the Aegean orocline thus rotated simultaneously: our new age constraints of 16–5 Ma in the east, compare with (largely) 15–8 Ma in the west, as published previously. The rotation of the Bey Dağları was probably bounded in the south at the plate boundary with Africa, and in the east by the Aksu thrust and Kırkkavak dextral strike-slip fault, which together partitioned dextral transpression induced by the rotating block. Accommodation of the western Anatolian rotations to the north and west of the Bey Dağları will be the subject of a future publication.

Key Words: Aegean, orocline, palaeomagnetism, IRM component analysis, remagnetization

Beydağları'nın Miyosen'de Yeniden Mıknatıslanmasının Test Edilmesi: Türkiye Güneybatısındaki Neojen Rotasyonlarının Zamanı ve Miktarı

Özet: Bu çalışma Ege oroklinalinin güneybatı Türkiye'deki doğu kanadı rotasyonunun zamanı ve miktarını yeniden değerlendirmektedir. Bu oroklinal için geçerli güncel model, Geç Kretase–Eosen yaşlı platform karbonatları ile Alt Miyosen filiş çökellerinin yüzlekler verdiği Beydağları bölgesinin saatin tersi istikamette 25–30°'lik bir açı ile döndüğü şeklindedir. Bu modele göre rotasyon Miyosen yeniden mıknatıslanmasından sonra meydana gelmiş olup, Ege orokliniinin batı ve doğu kanatları rotasyonlarının farklı zamanlarda gerçekleşmiş olabileceği gerçeğini dışlamaz. Bu modeli test etmek amacıyla, Beydağları Alt Miyosen istiflerinde ayrıntılı paleomanyetik çalışma icra edilmiştir.

Korkuteli ve Doğantaş civarında, Beydağları kireçtaşları ile uyumsuzluk gösteren Akitaniyen birimler ile başlayıp Üst Burdigaliyen–Alt Langiyen'a kadar uzanan Miyosen ön-ülke havza stratigrafisine sahip iki kompozit kesit örneklenmiş ve zengin bir paleomanyetik analiz veri gurubu elde edilmiştir.

Akitaniyen kireçtaşları ile Burdigalian mavi renkli killerdeki Kalıntı Doğal Mıknatıslanma (KDM) baskın olarak magnetit ve ikincil olarak grigayt ile hematite bağlıdır. Pozitif Terselme Testi, kalıntı doğal mıknatıslanma (KDM) kazanıldıktan sonra yeğince kompaksiyona uğramış olan örneklerden elde edilen polarite verilerinin jeomanyetik polarite zaman çizelgesi ile uyumlu oluşu, güvenli bir şekilde paleo-seküler değişime atfedilebilecek KDM yönlerindeki saçılım ile son zamanlarda önerilen ve eşsıcaklık ısıl kalıntı mıknatıslanma (EIKM) kazanım eğrilerinin test edildiği Uç Eleman Model Test sonuçlarının pozitif olması hep birlikte Beydağları Platfomu Miyosen çökellerinin yeniden mıknatıslanma geçirmediği sonucuna işaret etmektedir.

Var olan verilerin kısmen yeniden değerlendirilmesi yanında bizim sonuçlarımız, Beydağları bölgesinin Geç Kretase ile Geç Burdigaliyen arasında herhangi bir rotasyona uğramadığı, günümüzden 16 ile 5 My önce, yani Orta–Geç Miyosen aralığında ve daha önceden kaydedildiği üzere, Antalya'nın kuzeyindeki rotasyona uğramamış Pliyosen çökellerin depolanmasından önce ki dönemde, saatin tersi yönde 20°'lik bir rotasyona maruz kaldığına işaret etmektedir. Doğu kanat için önerdiğimiz 16–5 My'lik yeni yaş sınırlamamız ile (genel olarak) batı kanat için daha önceden yayınlanmış olan 15–8 My karşılaştırıldığında Ege oroklinalinin doğu ve batı kanatlarının eşzamanlı olarak rotasyona maruz kaldıkları sonucu ortaya çıkar. Beydağları'nın rotasyonu, muhtemelen güneyde Afrika levha sınırı ile, doğuda ise blok rotasyonlarına bağlı ortaya çıkan ve sağ yönlü transpresyonu paylaşan Aksu bindirmesi ile sağ yönlü Kırkkavak Fayı ile sınırlanmıştır. Batı Anadolu'nun Beydağları'nın kuzeyinde ve batısındaki rotasyonları ise gelecekteki yayınların konusu olacaktır.

Anahtar Sözcükler: Ege, oroklinal, paleomanyetizma, izotermal kalıntı mıknatıslanma bileşen analizi, yeniden mıknatıslanma

Introduction

The Aegean region fits the description of an orocline (Carey 1958): a pre-existing, roughly east–west-striking nappe stack (Aubouin 1957; Jacobshagen 1986; van Hinsbergen *et al.* 2005a) underwent ~50° clockwise (CW) rotation in the west (Kissel & Laj 1988; van Hinsbergen *et al.* 2005b) and reportedly ~30° counterclockwise (CCW) rotation in the east (Kissel & Poisson 1987; Morris & Robertson 1993), leading to the present-day arc shape (Figure 1).

Several geodynamic processes have been postulated to contribute to the formation of this orocline, which is amongst the best documented examples in the world. Most authors follow the explanation of Kissel & Laj (1988), in which back-arc extension in central Greece has led to vertical axis block rotations on either side of the arc. However, the onset of rotation in the western limb of the orocline (after ~15 Ma according to van Hinsbergen *et al.* 2005b) is much younger than the onset of back-arc extension dated ~25 Ma (Jolivet 2001; Tirel *et al.* 2009) or even older (Forster & Lister 2009). Alternative models incorporate contributions from the westward extrusion of Anatolia (Taymaz *et al.* 1991) or rotation due to a reconnection of the edge of the western Aegean domain with the African plate (van Hinsbergen *et al.* 2008).

The key to identifying the driving geodynamic mechanism behind the Aegean oroclinal bending lies in the determination of the age and kinematics of the rotating limbs of the orocline. The timing and sense and scale of rotations in the western (Horner & Freeman 1983; Kissel & Laj 1988; van Hinsbergen *et al.* 2005b), northern (van Hinsbergen *et al.* 2008) and southern (Duermeijer *et al.* 1998; van Hinsbergen *et al.* 2007) parts of the Aegean orocline are now well-defined, but the timing and amount of rotation in the eastern limb are still subject to discussion.

The eastern limb of the Aegean orocline lies in western Turkey (Figures 1 & 2) and is formed by the Bey Dağları carbonate platform – the deepest non-metamorphosed structural unit of western Anatolia (Şengör & Yılmaz 1981; Collins & Robertson 1998), overthrust in the east and west by the Antalya Nappes (in the Palaeocene, and later again in the middle to late Miocene) and the Lycian Nappes (in the early Miocene), respectively (Ricou *et al.* 1975; Poisson 1977; Robertson & Woodcock 1980; Hayward 1984c; Marcoux *et al.* 1989; Collins & Robertson 1998; Figure 2).

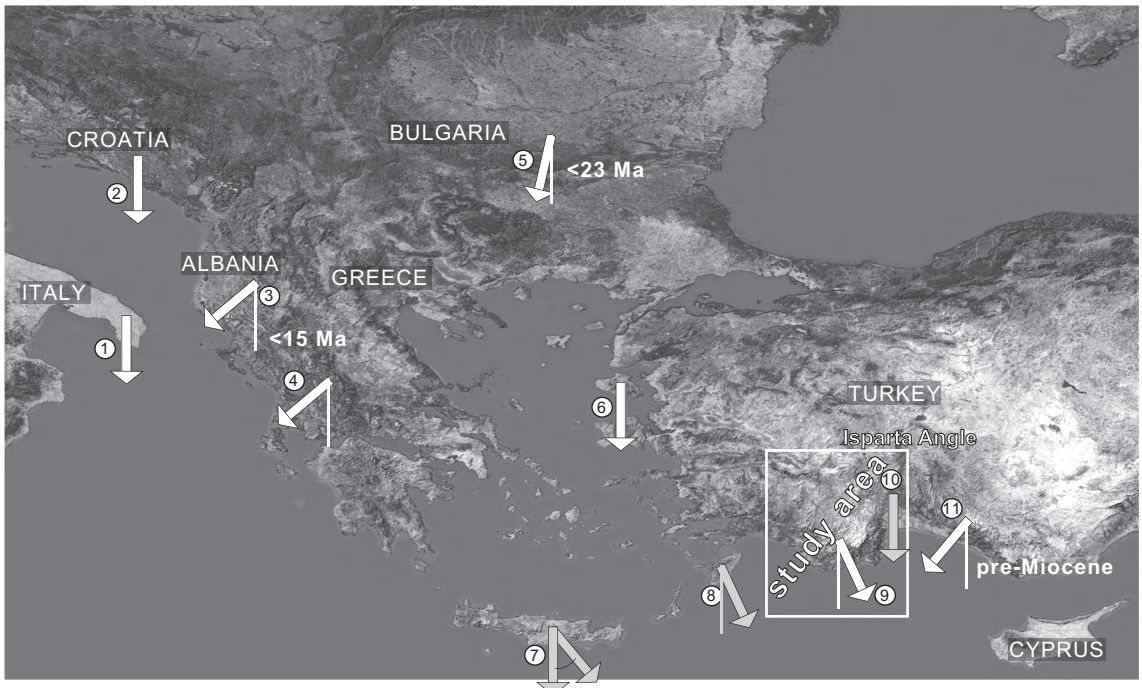

Figure 1. Topographic image of the eastern Mediterranean region (blue marble data set, see Stöckli *et al.* 2005). Arrows represent a selection of the most important reported declinations with respect to the south, giving the outline of the Aegean orocline, which runs from northern Albania to the Isparta Angle. White arrows represent directions measured in lower Miocene and older rocks, black arrows represent late Miocene and younger directions. 1– Apulian platform, no or little rotation since Eocene (Tozzi *et al.* 1988; Scheepers 1992; Speranza & Kissel 1993); 2– Dinarids, no rotation since the Cretaceous (Kissel *et al.* 1995); 3– Albania, ~50° of rotation since the early Miocene (Speranza *et al.* 1992, 1995; Mauritsch *et al.* 1995, 1996); 4– Western Greece and Peloponnese, ~50° clockwise rotation since the early Miocene (Horner & Freeman 1982, 1983; Kissel *et al.* 1984, 1985; Kissel & Laj 1988; Marton *et al.* 1990; Morris 1995; van Hinsbergen *et al.* 2005b); 5– Moesian platform and Rhodope, no significant post-Eocene rotation with respect to the Eurasian APWP (van Hinsbergen *et al.* 2008); 6– Lesbos, no significant rotation of Miocene volcanics (Kissel *et al.* 1989; Beck *et al.* 2001); 7– Crete, local, variable, strike-slip related post-Messinian counterclockwise rotations (Duermeijer *et al.* 1998); 8– Rhodes, Pleistocene counterclockwise rotation, but no rotation between the early Miocene and Pleistocene (Laj *et al.* 1982; van Hinsbergen *et al.* 2007); 9– Bey Dağları, counterclockwise rotations (Kissel & Poisson 1987; Morris & Robertson 1993), the timing and amount of which are discussed in this paper; 10– Isparta Angle, no Pliocene or younger rotations in its centre (Kissel & Poisson 1986); clockwise rotations between the Eocene and Miocene of the eastern limb of the Isparta Angle, delimiting the eastern edge of the Aegean orocline (Kissel *et al.* 1993).

Kissel & Poisson (1987) were the first to carry out palaeomagnetic analyses of the Bey Dağları platform. They resolved ~25° CCW rotation from Eocene and lower Miocene sediments. Morris & Robertson (1993), aiming to reconstruct the convergence history in SW Anatolia, analysed Cretaceous and lower Cenozoic rocks from the Bey Dağları carbonate platform, as well as Palaeozoic and Mesozoic sediments and effusive rocks of the Antalya Nappes and Taurides, and confirmed ~30° of CCW rotation. However, because they consistently found 30° northwesterly declinations throughout the Palaeozoic of the intensely deformed Antalya Nappes as well, they argued for a regionally pervasive remagnetization event related to a chemical remanent magnetization as a result of magnetite precipitation from orogenic fluids. Although they acknowledge that this remagnetization event could be related to the original Palaeocene emplacement of the Antalya Nappes, they favoured a middle to late Miocene remagnetization age, related to their inferred age of emplacement of the Lycian Nappes.

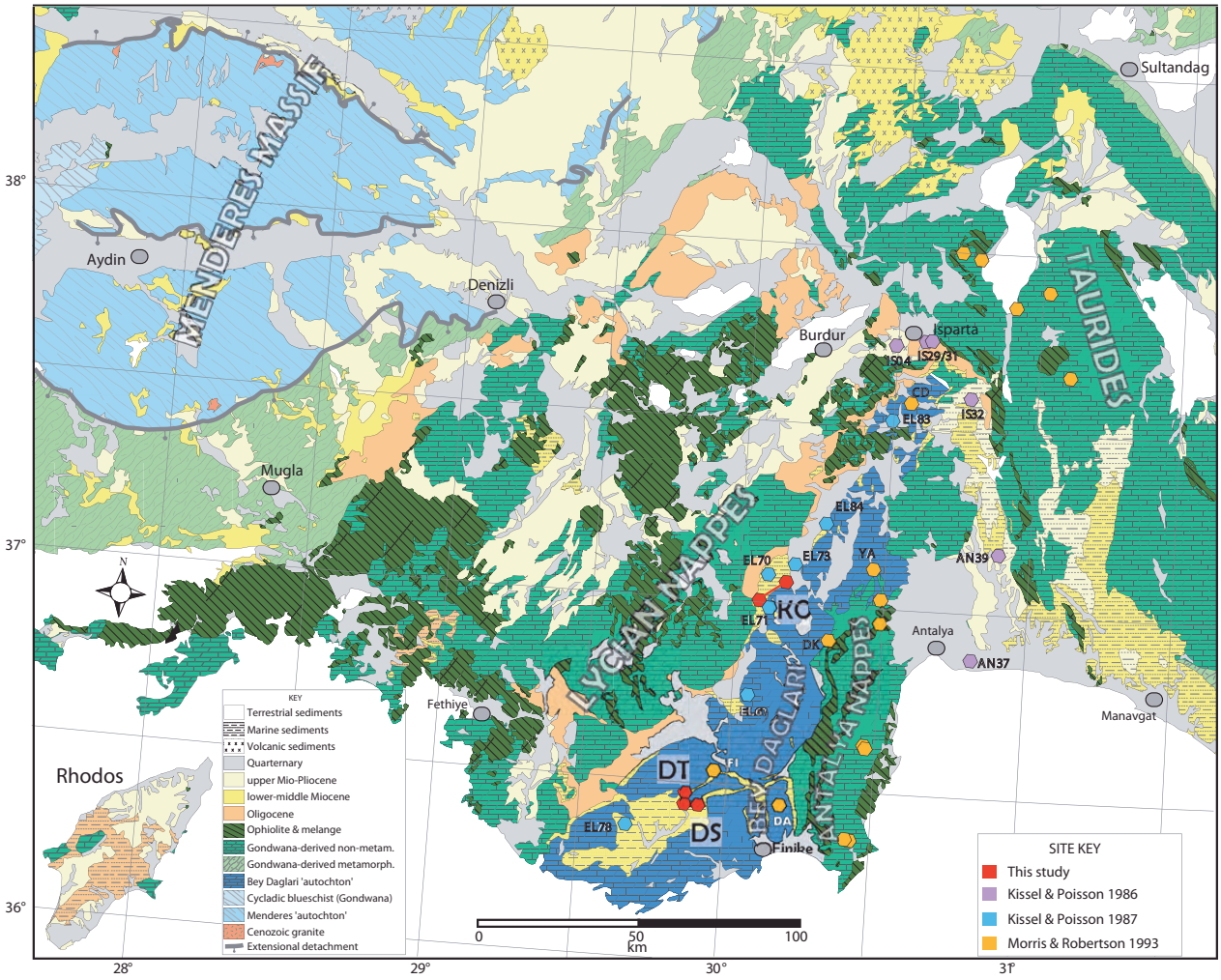

Figure 2. Geological map of southwestern Turkey, with sample locations, modified after Şenel (2002).

Thus the current model for the evolution of this orocline implies a 25–30° CCW rotation in southwestern Anatolia contemporaneous with the 50° CW rotation in western Greece. If there was indeed a middle Miocene remagnetization event in southwestern Anatolia, however, rotations here may have started much earlier, making the rotation history of the Aegean oroclinal limbs asynchronous, and the Bey Dağları rotation could then have been much larger, but partially obscured due to the remagnetization event.

Therefore, whether or not the Bey Dağları region is remagnetized warrants further investigation, along with the inferred middle–late Miocene remagnetization age. To this end we collected samples from two long (composite) sections in the lower Miocene succession covering the Bey Dağları platform. Our new results with a reassessment of some of the arguments of Morris & Robertson (1993) lead to a refinement of the kinematic history of Bey Dağları within the context of the development of the Aegean orocline.

Geological Setting

The Aegean and Cyprus arcs, or oroclines, intersect in southwestern Turkey (Figure 1). The junction between these arcs forms the so-called Isparta Angle (Blumenthal 1963), which is characterised by a long-term polyphase deformation history (Robertson

1993; Glover & Robertson 1998a; Poisson *et al.* 2003b; Robertson *et al.* 2003; Zitter *et al.* 2003; ten Veen *et al.* 2004). The eastern limb of the Isparta Angle is formed by the Taurides fold and thrust belt, rotated ~40° clockwise between the Eocene and the early Miocene (Kissel *et al.* 1993). The western limb consists of the Bey Dağları carbonate platform which is overthrust in the northwest by the Lycian Nappes (Hayward 1984c; Collins & Robertson 1998). The centre of the Angle is occupied by the Antalya Nappes that overthrust both the Bey Dağları platform to the west and the Taurides to the east (Poisson *et al.* 2003b; Robertson *et al.* 2003). In addition, the Isparta Angle hosts a series of Neogene sedimentary basins (Figure 2).

The Bey Dağları carbonate platform is at present a NE–SW-striking anticlinorium (Figure 2) that exposes mainly Cretaceous to Eocene, and locally Oligocene, platform and pelagic carbonates (Poisson 1967, 1977; Farinacci & Köylüoğlu 1982; Hayward & Robertson 1982; Sarı & Özer 2002; Sarı *et al.* 2004, 2009).

The Lycian Nappes formed as a result of accretion during late Cretaceous to Eocene intra-oceanic and subsequent continental subduction. They consist of an ophiolite, ophiolitic mélange and stacked deep to shallow marine passive margin sediments (de Graciansky 1972; Bernoulli *et al.* 1974; Poisson 1977; Okay 1989; Collins & Robertson 1997, 1998, 2003) that underwent high-pressure and low-temperature metamorphism in the north but remained unmetamorphosed in the south (Candan *et al.* 2001; Rimmelé *et al.* 2003, 2006). Following stacking, the Lycian Nappes were underthrust after the Palaeocene (Özer *et al.* 2001) by the Menderes Massif, which is generally considered to belong to the same continental lithospheric block as the Bey Dağları platform (Şengör & Yılmaz 1981; Collins & Robertson 1998). Since the late Oligocene, the Menderes Massif has been exhumed as a sequence of symmetrical up-domed core complexes (Bozkurt & Park 1994; Hetzel *et al.* 1995a; Bozkurt & Satır 2000; Bozkurt 2004, 2007) and the Lycian Nappes have been translated southwards over the Bey Dağları platform (Collins & Robertson 1998).

As a result of the southward translation of the Lycian Nappes, the Bey Dağları platform subsided isostatically and a Miocene foreland basin developed, covering most of the platform (Hayward 1984c; Kosun *et al.* 2009). This basin includes sub-basins, such as the Dariören basin immediately in front of and below the Lycian Nappes thrust stack, and the Kasaba syncline and the Çatallar basin further to the south (Figure 2). Sedimentation in these basins commenced in the Aquitanian with shallow marine reef limestones and subsided in the Burdigalian to several hundreds of metres depth, while being filled with marls and mass-flow deposits (de Graciansky 1972; Poisson 1977; Gutnic *et al.* 1979; Hayward 1984c; Koşun *et al.* 2009). The recognition of a window in the Lycian Nappes with Burdigalian flysch near Göcek (Brunn *et al.* 1970; Hayward 1984b), ~75 km away from the present-day thrust front provides a minimum Miocene translation distance for the Lycian Nappes.

Thrusting of the Lycian Nappes over the Dariören basin stopped in the Langhian. This is constrained by (1) the age of the youngest deposits below the thrust in the Dariören basin (Langhian: Hayward 1984b); (2) the presence of proximal, Lycian Nappes-sourced fan delta conglomerates at the top of the succession (Poisson 1977; Gutnic *et al.* 1979; Hayward *et al.* 1996; Karabıyıkoğlu *et al.* 2005) and (3) Serravallian sediments in the Aksu Basin (see below) unconformably covering a thrust fault between the Kapıkaya Block, correlated with the Lycian Nappes, and Burdigalian and Langhian sediments (Poisson *et al.* 2003b; Flecker *et al.* 2005).

Following the end of thrusting of the Lycian Nappes, the Bey Dağları region formed an uplifting piedmont and was covered by Serravallian and possibly Tortonian upward-shallowing marine and terrestrial sediments shed from the Lycian Nappes, and, locally in the southeast, from the Antalya Nappes (Hayward & Robertson 1982; Hayward 1983, 1984b, c; Hayward *et al.* 1996; Koşun *et al.* 2009). Probably during the late Miocene, the Bey Dağları Platform was folded into the present anticlinorium, and the Miocene foreland basin was dissected by the E–W-trending, south-verging Susuzdağ thrust (Uysal *et al.* 1980; Şenel 1997), which isolates the Kasaba syncline and the Çatallar basin from the Dariören basin (Hayward 1984c; Koşun *et al.* 2009).

In the east, the Bey Dağları platform was overthrust by the Antalya Nappes, comprising a

series of Palaeozoic and Mesozoic passive margin sediments and an ophiolite (Juteau *et al.* 1977; Gutnic *et al.* 1979; Robertson & Woodcock 1980, 1981a, b, c, 1982, 1984; Reuber *et al.* 1982; Bağcı & Parlak 2009). The ages of metamorphic soles, indicating the age of onset of obduction, of the ophiolites of the Lycian Nappes, the Antalya Nappes, and others throughout the Taurides are all virtually the same, i.e. 94–90 Ma (Dilek & Whitney 1997; Parlak & Delaloyle 1999; Önen & Hall 2000; Çelik *et al.* 2006; Çelik 2008; see also Moix *et al.* 2008). This is consistent with a common provenance in the north as advocated by Ricou *et al.* (1975) and Marcoux *et al.* (1989). However, most authors prefer the Antalya Nappes and ophiolite to have originated from a separate oceanic branch of the Neotethys south of the Taurides (Dumont *et al.* 1972; Şengör & Yılmaz 1981; Poisson 1984; Robertson 1993; Poisson *et al.* 2003b; Vrielynck *et al.* 2003; Moix *et al.* 2008).

The emplacement of the Antalya Nappes over the Bey Dağları platform to the west, and over Mesozoic to Palaeogene carbonates of the Taurides to the east (Figure 2) occurred initially in the Palaeocene (Poisson 1977; Poisson *et al.* 2003b). Later, in middle to late Miocene times, out-of-sequence thrusting led to further westward emplacement of the Antalya Nappes over the Bey Dağları platform, possibly with a strike-slip component (Hayward & Robertson 1982; Hayward 1984a, b; Poisson *et al.* 2003b).

The central and eastern parts of the Isparta Angle expose the Neogene sedimentary basins of Manavgat, Köprü (or Köprüçay) and Aksu. These subsided in the middle Burdigalian, with stratigraphic successions resembling, but consistently younger than those on top of the Bey Dağları Platform to the west. They start with conglomerates and reefs, followed by more distal marl and mass-flow dominated deposits in the Langhian to Tortonian, with these basins receiving sediments until the Pliocene (Bizon *et al.* 1974; Akay & Uysal 1981; Akay *et al.* 1985; Flecker *et al.* 1995, 1998; Poisson *et al.* 2003a; Karabıyıkoğlu *et al.* 2005; Çiner *et al.* 2008). The Köprü and Aksu basins formed originally as half-grabens in the early Miocene, and were subjected to folding during late Miocene dextral transpression; in the Aksu basin this led to westward thrusting (Dumont & Kerey 1975; Poisson 1977; Frizon de Lamotte *et al.* 1995; Glover & Robertson 1998a; Deynoux *et al.* 2005; Çiner *et al.* 2008) which continued until the late Miocene (Glover & Robertson 1998a) or Pliocene (Poisson *et al.* 2003a).

The Plio–Pleistocene history of the Antalya Basin, finally, was latterly dominated by NE–SW extension (Price & Scott 1994; Cihan *et al.* 2003; Glover & Robertson 2003; ten Veen 2004; Alçiçek 2007) inferred by several authors to occur in the rear of the left-lateral Pliny and Strabo trenches of the southern Aegean system (Dumont *et al.* 1979; Price & Scott 1994; Barka & Reilinger 1997; Glover & Robertson 1998a, b; ten Veen *et al.* 2009), which came into existence during the early Pliocene (Woodside *et al.* 2000; van Hinsbergen *et al.* 2007; Zachariasse *et al.* 2008).

Sections and Methods

Sampled Sections

Kissel & Poisson (1986, 1987) and Morris & Robertson (1993) published successful palaeomagnetic results from 13 sites across the Bey Dağları, with ages ranging from late Cretaceous to early Miocene, as well as from five sites in Pliocene and younger sediments in the Isparta Angle (Table 1, Figure 2). The regional distribution of rotations is therefore reasonably well determined, and our sampling focused on collecting palaeomagnetic information from coherent lower to middle Miocene successions, in order to test whether these are remagnetized, and whether they were deposited before, during or after the previously estimated 25–30° CCW rotation phase.

To this end, we sampled a ~1500-metre-thick section near Korkuteli (Figures 2 & 3), which spans a continuous Miocene stratigraphy in the Dariören basin, from the unconformity between the Eocene Bey Dağları limestones, up to the tectonic mélange below the thrust of the Lycian Nappes (Figure 4). According to previous work (Poisson 1977; Gutnic *et al.* 1979; Hayward 1984b; Hayward *et al.* 1996; Karabıyıkoğlu *et al.* 2005), the age of the Korkuteli section ranges from Aquitanian to early Langhian. We collected 336 samples at 86 levels throughout the stratigraphic successions, with three samples at every

Table 1. New (upper pane) and previous (lower pane) palaeomagnetic results for the Bey Dağları. For locations of the sites and sections, see Figure 2. Lat– latitude of the site, Lon– longitude of the site. For the sections, the coordinate of the base of the section is given. Coordinates for the published sites are estimated, based on the maps in the original publications; Na– number of samples analysed; Nc/vD– number of samples used in the calculation of the average, which, for the new results, were not excluded by the Vandamme (1994) cut-off; D– declination, ΔD_x– 95% confidence interval on the declination, following Butler (1992); I– inclination, ΔI_x– 95% confidence interval on the inclination, following Butler (1992); $K_{(vgp)}$– Fisher precision parameter on the virtual geomagnetic pole; $A95_{(vgp)}$– 95% cone of confidence on the virtual geomagnetic pole; $k_{(dir)}$– Fisher precision parameter of the palaeomagnetic direction; $\alpha95_{(dir)}$– 95% cone of confidence of the palaeomagnetic direction; $A95_{min/max}$– lower/upper limit of possible palaeosecular variation induced A95 values following Deenen *et al.* (submitted). Notes: * values for the Korkuteli section after flattening correction using the E/I method of Tauxe & Kent (2004); only normal directions from blue clay samples were used (see text); ** to average the published datasets, we have parametrically resampled the published sites, converting the α95 to A95 using the conversion formula of Deenen *et al.* (submitted). We prefer this procedure above averaging site averages because this way we include the level to which PSV is averaged in our means and error bars; *** site rejected due to negative fold test, see text and Morris & Robertson (1993); **** in the original publications the K and A95 values of the VGPs was not given. We have recalculated these following the A95/α95 conversion formula given in Deenen *et al.* (submitted); ***** in the original publications of Kissel & Poisson (1986, 1987), the α95 values are not consistent with the given N and k values. We have recalculated the α95 values.

Locality				Nc/v	Tilt corrected									sedimentary		Age	Reference
Lava / neck site	Lat	Lon	Na	D	D	DDx	I	DIx	K(vgp)	A95(vgp)	k(dir)	a95(dir)		A95min	A95max	Ma	
Korkuteli*	37.0473	30.1425	**340**	**192**	**339.5**	**2.5**	**45.5**	**2.7**	**22.0**	**2.2**				**2.3**	**3.0**	**early–middle Miocene**	
Korkuteli (without E/I correction)			340	261	340.4	2.1	33.5	3.1	20.0	2.0				2.1	2.4		This study
normal				213	340.1	2.2	33.8	3.2	23.1	2.1				2.2	2.8		This study
reversed				49	161.7	6.8	-33.7	10.0	10.9	6.5				3.6	7.6		This study
Doğantaş	36.4514	29.8567	**139**	**36**	**327.8**	**9.0**	**47.7**	**9.3**	**10.1**	**7.9**				**4.0**	**9.4**	**early–middle Miocene**	
normal				30	325.1	10.0	47.2	10.4	10.0	8.8				4.2	10.6		This study
reversed				6	161.5	23.8	-49.2	23.3	11.7	20.4				7.2	31.8		This study
Doğantaş I			*35*	*4*	*347.4*	*18.3*	*41.7*	*22.2*	*31.5*	*16.6*			*n*	*8.2*	*41.9*		This study
Doğantaş II			*38*	*22*	*320.2*	*11.8*	*48.1*	*12.0*	*10.0*	*10.3*			*n/r*	*4.7*	*13.1*		This study
Doğantaş III			*61*	*12*	*330.5*	*16.3*	*42.9*	*19.3*	*9.6*	*14.8*			*n/r*	*5.7*	*19.8*		This study
Published data - averages of parametrically sampled directions																	
upper Cretaceous – Palaeogene**			**58**	**52**	**341.9**	**4.6**	**39.5**	**5.9**	**22.7**	**4.2**				**3.5**	**7.3**	**l. Cretaceous – Paleogene**	
Miocene**			**34**	**33**	**338.0**	**6.2**	**41.5**	**7.7**	**19.7**	**5.7**				**4.1**	**10.0**	**early–middle Miocene**	
Pliocene–lower Pleistocene**			**43**	**42**	**5.8**	**4.1**	**53.3**	**3.5**	**61.1**	**3.4**				**3.8**	**8.5**	**Pliocene–early Pleistocene**	
									calculated****								
DA	36.4467	30.1840		4	344.0		44.0		36.1	15.5	40.0	14.7		8.2	41.9	Paleocene	Morris & Robertson 1993
FI	36.5287	29.9521		12	354.0		40.0		28.3	8.3	30.0	7.9		5.7	19.8	Paleocene	Morris & Robertson 1993
DK	36.9104	30.3213		8	349.0		45.0		19.1	13.0	21.0	12.3		6.5	26.1	Paleocene	Morris & Robertson 1993
CD	37.5757	30.5586		5	352.0		42.0		19.4	17.8	21.0	16.9		7.6	36.0	late Cretaceous – Palaeogene	Morris & Robertson 1993
YA***	37.0228	30.4890		27	312.0		39.0		13.7	7.8	15.0	7.4		4.4	11.4	late Cretaceous – Palaeogene	Morris & Robertson 1993
EL 71	37.0517	30.1782		8	340.0		54.0		48.9	8.0	54.0	7.6	*****	6.5	26.1	Eocene	Kissel & Poisson 1987
EL 84	37.2315	30.2904		8	154.0		-29.0		55.5	7.5	61.0	7.1	*****	6.5	26.1	Eocene	Kissel & Poisson 1987
EL 83	37.5255	30.4956		6	115.0		-16.0		17.0	16.7	19.0	15.8	*****	7.2	31.8	Eocene	Kissel & Poisson 1987
EL 67	36.7661	29.9794		7	333.0		40.0		50.2	8.6	55.0	8.2	*****	6.8	28.6	Oligocene	Kissel & Poisson 1987
EL 78	36.4445	29.7382		7	359.0		68.0		35.3	10.3	39.0	9.8	*****	6.8	28.6	early–middle Miocene	Kissel & Poisson 1987
EL 70	37.0347	30.1761		10	161.0		-30.0		34.0	8.4	37.0	8.0	*****	6.1	22.5	early–middle Miocene	Kissel & Poisson 1987
EL 73	37.1384	30.2375		9	324.0		39.0		50.7	7.3	57.0	6.9	*****	6.3	24.1	early–middle Miocene	Kissel & Poisson 1987
IS 32	37.4623	30.7812		8	352.0		43.0		146.0	4.6	163.0	4.4	*****	6.5	26.1	middle Miocene	Kissel & Poisson 1986
IS 29	37.7243	30.6728		8	5.3		59.0		152.5	4.5	170.0	4.3	*****	6.5	26.1	early Pleistocene	Kissel & Poisson 1986
IS 31	37.6792	30.7180		9	358.0		58.0		259.8	3.2	288.0	3.0	*****	6.3	24.1	early Pleistocene	Kissel & Poisson 1986
AN 37	36.8930	30.8535		9	186.0		-48.0		244.4	3.3	270.0	3.1	*****	6.3	24.1	late Pliocene	Kissel & Poisson 1986
IS 04	37.7153	30.5192		9	12.5		46.6		194.6	3.7	221.0	3.5	*****	6.3	24.1	early Pliocene	Kissel & Poisson 1986
AN 39	37.1415	30.8083		8	182.0		-52.0		17.3	13.7	19.0	13.0	*****	6.5	26.1	early Pliocene	Kissel & Poisson 1986

level. To increase the dataset, we collected 45 samples from three sites at the bottom of the section, as well as 45 at the topmost levels to ensure sufficient statistical power for inclination shallowing corrections using the method of Tauxe & Kent (2004).

Another 125 samples were collected from three sections near the village of Doğantaş in the Kasaba syncline (Figures 2 & 5). Section Doğantaş I contains 35 sample levels with one sample per level in white, fossiliferous limestones at the base of the Miocene succession; these levels were dated as Aquitanian by (Hayward 1984c; Figure 4). Section Doğantaş II starts near the top of the Aquitanian limestones, where 18 levels with a single specimen at each were sampled. The succeeding Burdigalian stratigraphy of clay and turbiditic sandstones (Hayward 1984c) was sampled at 7 levels, with 3–5 samples per level. These levels are in stratigraphic order, but separated by large unexposed intervals in a river bed, and we cannot exclude the possibility of repetition due to unexposed faults. Finally, 12 levels of 3–5 samples were collected from the Doğantaş III section, with 15 samples at the top level, taken below the Susuzdağ thrust in blue Burdigalian clays (Figure 4).

Palaeomagnetic and Supporting Rock-magnetic Methods

Samples were collected using a water-cooled, generator-powered electric drill, and oriented with a magnetic compass. They were cut into standard specimens of 1 inch diameter and 22 mm length; at least one specimen per core was demagnetized. 340 specimens, cut from 336 samples were analyzed from the Korkuteli section, and 139 specimens cut from 125 samples were measured from the Doğantaş section.

Demagnetization was mostly performed with alternating fields (AF) with 5–10 mT increments up to 100 mT, with a degausser interfaced with the magnetometer through a laboratory-built automated handling device. A selection of samples was thermally demagnetised with small temperature increments of 20–80 °C in a magnetically-shielded, laboratory-built furnace to check for consistency of directions between AF and thermal demagnetization. These directions appeared to be statistically indistinguishable. NRM (and isothermal remanent magnetization (IRM)) were measured on a 2G Enterprises horizontal DC-SQUID magnetometer (noise level 3×10^{-12}Am^2).

To support the palaeomagnetic interpretation various rock-magnetic properties were determined on selected samples. Thermomagnetic data were acquired with a modified horizontal translation type Curie balance that uses a cycling field between 150 and 300 mT rather than a fixed applied field (Mullender *et al.* 1993; noise level ~4×10^{-9} Am^2). About 40 mg of sample material was weighed in a quartz glass sample holder. To discriminate between magnetic behaviour and chemical alteration we applied the so called segmented run protocol in which heating is applied to a certain temperature followed by cooling of 100 °C before heating to the next temperature. Magnetic behaviour is documented by reversible heating and cooling branches while chemically-induced changes up to the temperature of interest are manifested by irreversible magnetic behaviour. Segment temperatures are 250, 350, 450, 520, 620 and 700 °C (so cooling to subsequently, 150, 250, 350, 450, 500 °C and back to room temperature after heating to 700 °C). The somewhat noisy appearance of the thermomagnetic curves testifies to the low signals involved.

IRM acquisition curves were measured up to 700 mT with 57 steps and 49 curves were acquired, using the robotized 2G Enterprises SQUID magnetometer with in-line AF demagnetization, ARM and IRM acquisition facilities. IRM acquisition was done from the so-called AF demagnetized starting state: prior to the IRM acquisition the samples were demagnetized in three orthogonal axes at 300 mT AF with a laboratory-built demagnetization coil. This ensures that the shape of the measured IRM acquisition curves deviates minimally from a cumulative log-Gaussian distribution (cf. Heslop *et al.* 2004).

A few hysteresis loops (between ±2 Tesla) were determined with a MicroMag 2900 alternating gradient magnetometer (Princeton, USA, noise level ~4×10^{-11} Am^2). Averaging time for each data point was 0.2 sec and the field increment between subsequent data points was 10.0 mT. Most samples

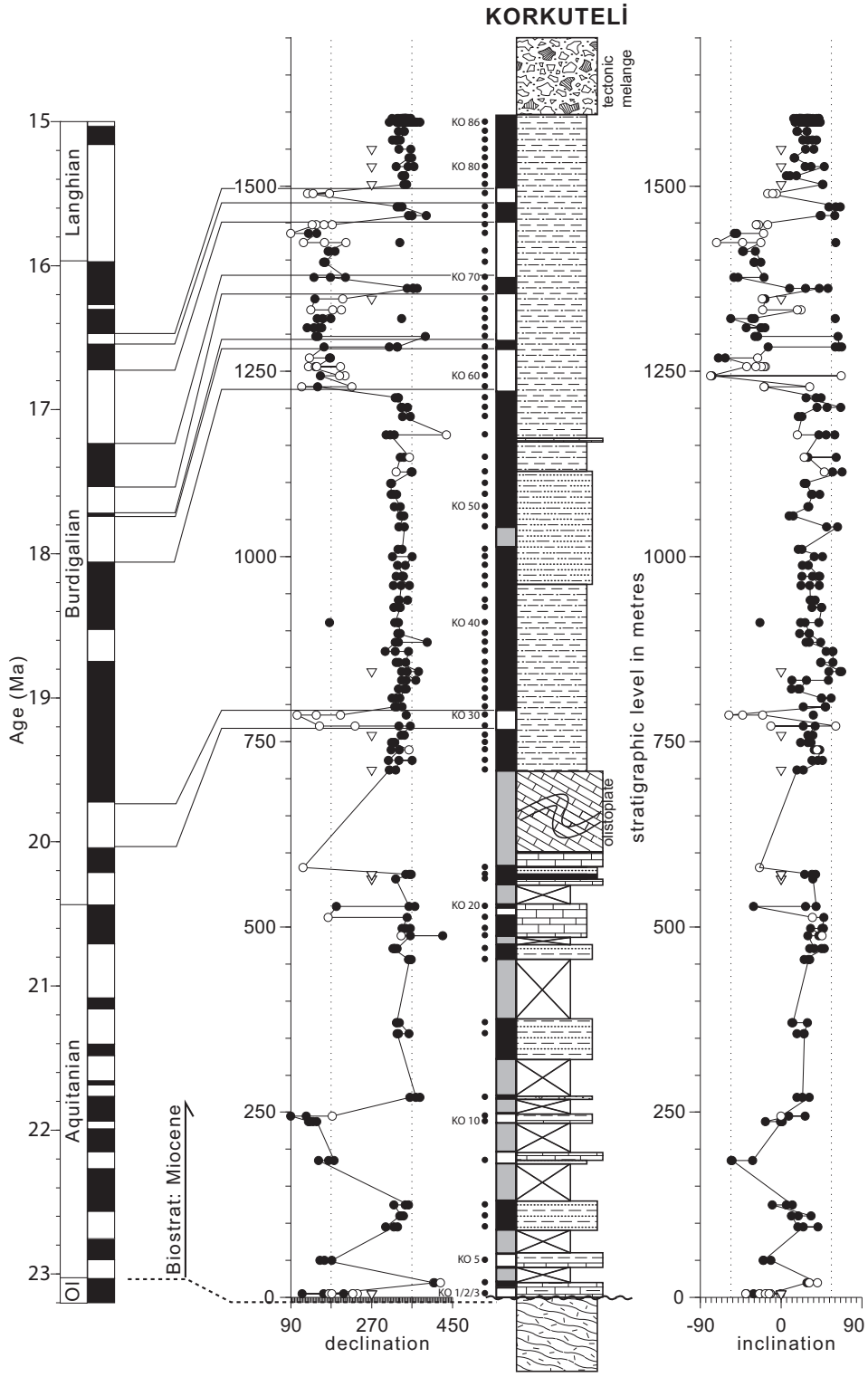

Figure 3. Schematic log of the Korkuteli section, with sample levels, palaeomagnetic results and magnetostratigraphic interpretation, with normal (black), reversed (white) or undetermined (grey) polarity. Closed (open) circles are type 1 (2) quality directions; open triangles gave no sensible palaeomagnetic result (type 3); see text. Geomagnetic polarity timescale taken from Lourens *et al.* (2004). For Key, see Figure 5.

Figure 4. Field photographs illustrating exposures and lithologies of the sampled sections. **(A)** Basal unconformity of the Korkuteli section, showing a NE tilted contact between Eocene limestones and Aquitanian marly limestones of the Dariören basin; **(B)** Burdigalian blue clays and thin turbidites of the Doğantaş III section. The white limestones at the top of the hill comprise the hangingwall of the Susuzdağ thrust and override the Burdigalian flysch; **(C)** Echinoid in the shallow marine Aquitanian limestones of the Doğantaş I section; **(D)** alternating blue clay and turbiditic sandstones that form the bulk of the Miocene stratigraphy of the Korkuteli section and **(E)** slump-folded limestones of the thick olistoplate around 650 m in the Korkuteli section (see Figure 3).

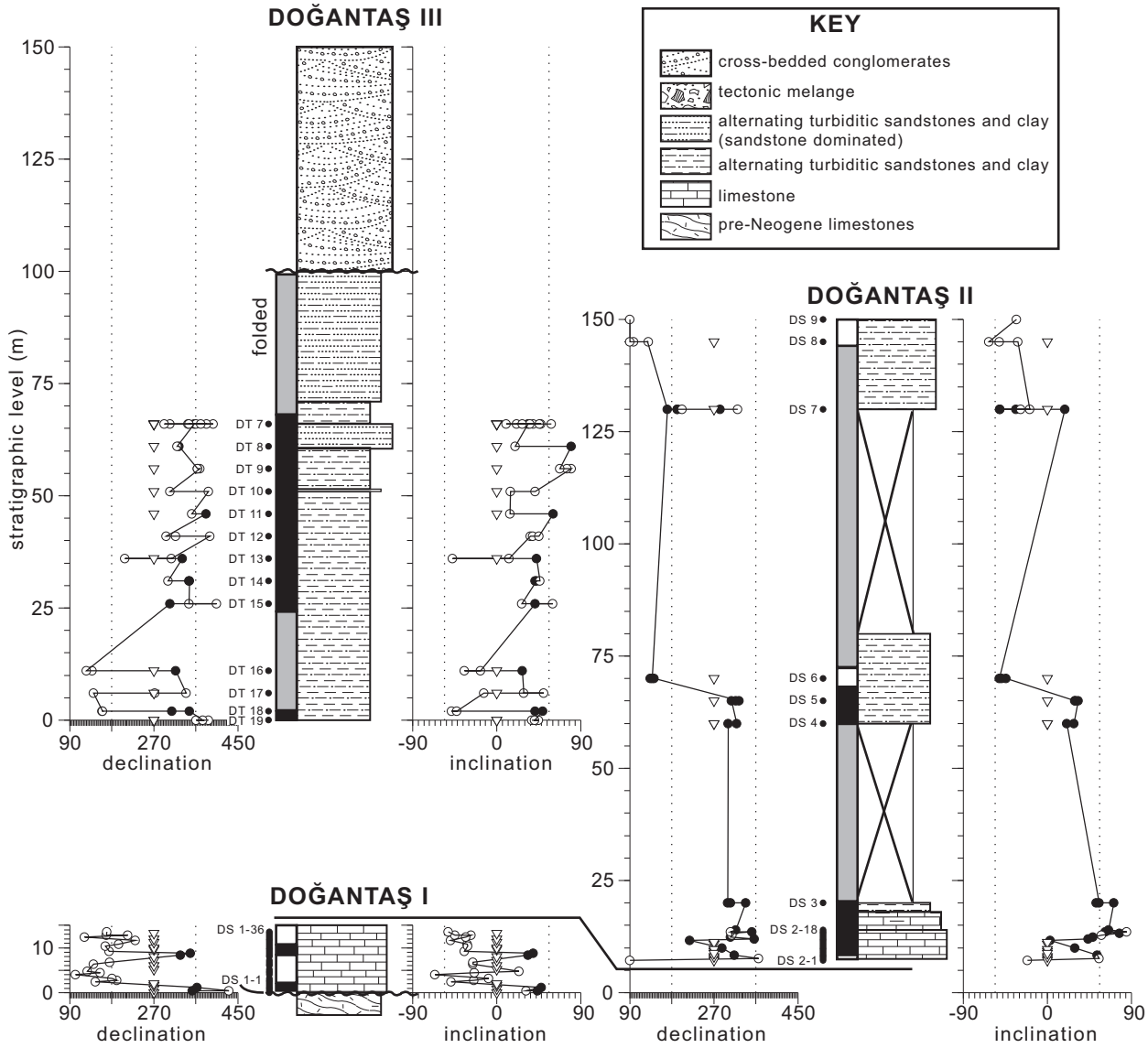

Figure 5. Schematic logs of the three sub-sections sampled near Doğantaş with sample levels, palaeomagnetic results and magnetostratigraphic interpretation, with normal (black), reversed (white) or undetermined (grey) polarity. Closed (open) circles are type 1 (2) quality directions; open triangles gave no sensible palaeomagnetic result (type 3); see text.

appeared to be weakly magnetic, which precluded determination of meaningful loops. The examples shown (Figure 7) correspond to the stronger samples.

Palaeomagnetic Results

First we describe the outcome of magnetic property analyses to constrain the magnetic mineralogy of the sample collection. This is followed by the palaeomagnetic interpretation.

Rock Magnetic Properties

Thermomagnetic Runs – Aquitanian limestone sample DS1-6B from section Doğantaş I (Figure 6A) is typical of the limestones under study. Most of the magnetization is due to the paramagnetic (plus

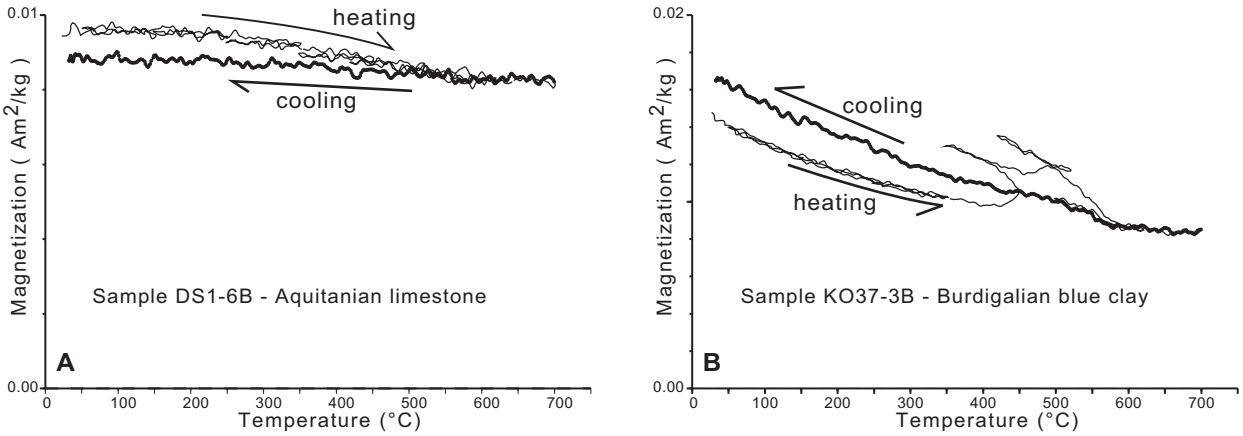

Figure 6. Thermomagnetic curves generated with the segmented heating protocol. The final cooling segment is indicated with the thicker black line. The noisy appearance testifies to the weak magnetic signals (in particular sample DS1-6B is weak). See text for explanation of the thermomagnetic behaviour.

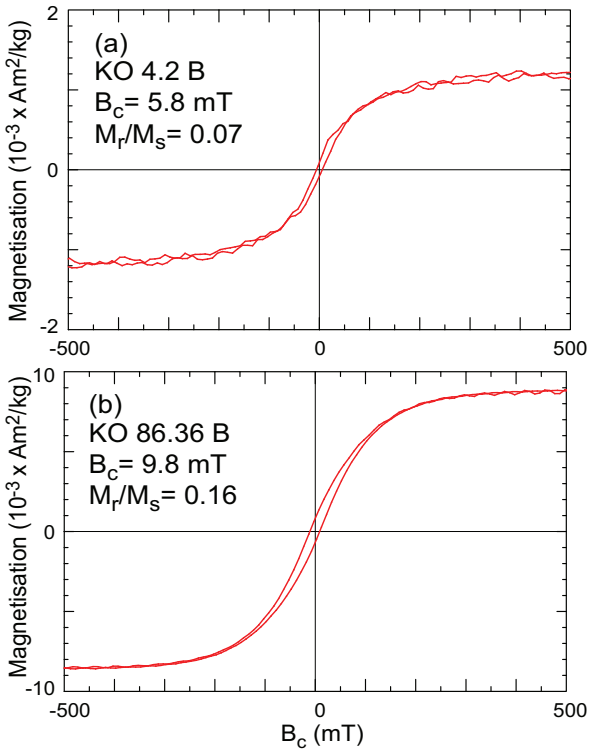

Figure 7. Examples of magnetic hysteresis loops corrected for the paramagnetic contribution. Only the central portion between ±500 mT is shown. Hysteresis parameters are indicated. KO4.2B is limestone, KO86.36 blue clay.

diamagnetic) matrix contribution; the sample contains only ~0.001 Am^2/kg ferromagnetic material which is here most probably a combination of partially maghemitized magnetite and approximately pure magnetite (if recalculated to pure magnetite it would imply an amount of ~10 ppm of magnetite). Magnetite presence is established from a Curie temperature of slightly below ~600 °C. Maghemitized magnetite is deduced from the small irreversible decrease between ~300 °C and 450 °C, a temperature interval where inversion of maghemitized magnetite to hematite occurs. Reaction of a magnetic sulphide (greigite) or pyrite is considered less likely because no increase in magnetization is noticed that results from the magnetite-like intermediate phase that occurs during the transition of greigite and/or pyrite to hematite (Passier *et al.* 2001; Vasiliev *et al* 2008; see also Figure 6B).

In the Burdigalian blue clay sample from the Korkuteli section (KO 37-1B; Figure 6B), which is slightly more magnetic than the limestone sample, the transition from pyrite via magnetite to hematite is noticed. Pyrite starts to react to form magnetite at 420 °C (Passier *et al.* 2001). This induces an increase in magnetization between 420 and ~600 °C. At about 500 °C the amount of magnetite is maximal as shown by the increase during cooling from 520 to 420 °C. During heating up to 620 °C part of the newly formed magnetite is transformed to hematite because the cooling segment to 500 °C is irreversible. The subsequent heating up to 700 °C does not induce further changes since the final cooling curve

duplicates the 620–500 °C segment. The Néel temperature of hematite is not really noticeable due to the minute amounts of hematite involved, but its generation is attested to by the slightly reddish color of the sample after treatment. The presence of magnetic sulphides cannot be deduced from the thermomagnetic curve – if present their amount is lower than the resolution of the instrument. The slightly more hyperbolic shape of the heating curve in comparison to that of the limestone sample indicates more paramagnetic minerals in the clay sample, as anticipated for clay that contains more detrital silicates than a carbonate. Also it is not possible to infer an estimate of how much magnetite was originally present in the sample: the amount of magnetite created due to the breakdown of the sulphide(s) significantly outweighs any magnetite that was potentially originally present.

Hysteresis Loops – The samples appeared to be magnetically very weak and dominated by the paramagnetic and diamagnetic matrix contributions. Typical examples of slope-corrected loops of a stronger Korkuteli limestone (KO4-2B) and a blue clay (KO86-36B) sample are shown in Figure 7. M_{rs}/M_s ranges between 0.07 and 0.16 and B_c between 6 and 10 mT. This indicates PSD grains with possibly a superparamagnetic contribution. Because the paramagnetic part of the loop is so large, slope correction appeared to be critical. After slope correction noisy loops resulted that cannot be interpreted meaningfully and further hysteresis loop determination had to be abandoned. Emphasis was put on the IRM acquisition curves that are much less influenced by instrumental noise level constraints.

Component Analysis of IRM Acquisition Curves – IRM curve fitting was done by interactively optimizing the fits in three representations of the data (all plotted against log-field): the IRM acquisition curve, the gradient of the curve and the standardized values of that curve. The first two representations are based on absolute values while the last is a relative representation that enables better visualization of the low- and high-field ends of the distribution (to optimize analysis of the effect of thermal activation and/or magnetic interaction, and the high-coercivity part of the distribution respectively). To account for skewed distributions as a consequence of magnetic interaction and/or thermal activation (see Egli 2003, 2004; Heslop *et al.* 2004) an extra coercivity component was fitted at the low-field end. This component (component 2 on Figure 8) is not given physical meaning and its amount (typically just a few per cent) was added to the dominant low-coercivity component (referred to as component 1 in Figure 8 and Table 2).

In Figure 8 four typical examples of the fits are shown: two of the Korkuteli section and two of the Doğantaş composite section. In both lithologies, the blue clays (eight samples) and limestones (44 samples), the dominant coercivity component, component 1, is characteristic of magnetite. The amount of 'component 2' needed to account for the skewed-to-the-left distribution as a consequence of thermal activation is just a few per cent. The blue clays appear to be close to magnetic saturation at 700 mT acquisition fields, the amount of a high coercivity component (component 3 in Figure 8; Table 2) to obtain good fits is typically a few per cent as well. Most limestone samples are close to saturation as well after application of the maximum available field of 700 mT. However, some samples at the base of the Korkuteli section (example KO 3-8B) are not saturated: they show an appreciable amount of a high-coercivity fraction interpreted to be hematite. Also some levels from the Doğantaş sections contain a fair amount of hematite, notably in the top few metres of the Aquitanian limestones. Note that in Table 2 the amounts and proportions of the complete distributions are tabulated. The measured part of the high-coercivity distribution is a only minor fraction of the total distribution. Extrapolation is done via the model of a cumulative log-Gaussian distribution for each coercivity component.

IRM component analysis reveals distinct differences in magnetic properties. The total SIRM ranges in the limestones from ~1×10^{-6} to ~2×10^{-4} Am^2kg^{-1}; not unexpectedly it is higher in the blue clays and varies from ~3.5×10^{-5} to ~2×10^{-3} Am^2kg^{-1}. In the Doğantaş limestones component 1 averages to $B_{1/2}$= 64.8 mT (+71.0 / –59.1 mT; this is asymmetric because the inverse logarithm is taken) with DP = 0.31±0.015 (log units). We interpret component 1 as detrital magnetite (*cf.* Kruiver & Passier 2001; Kruiver *et al.* 2003). $B_{1/2}$ is high for magnetite which

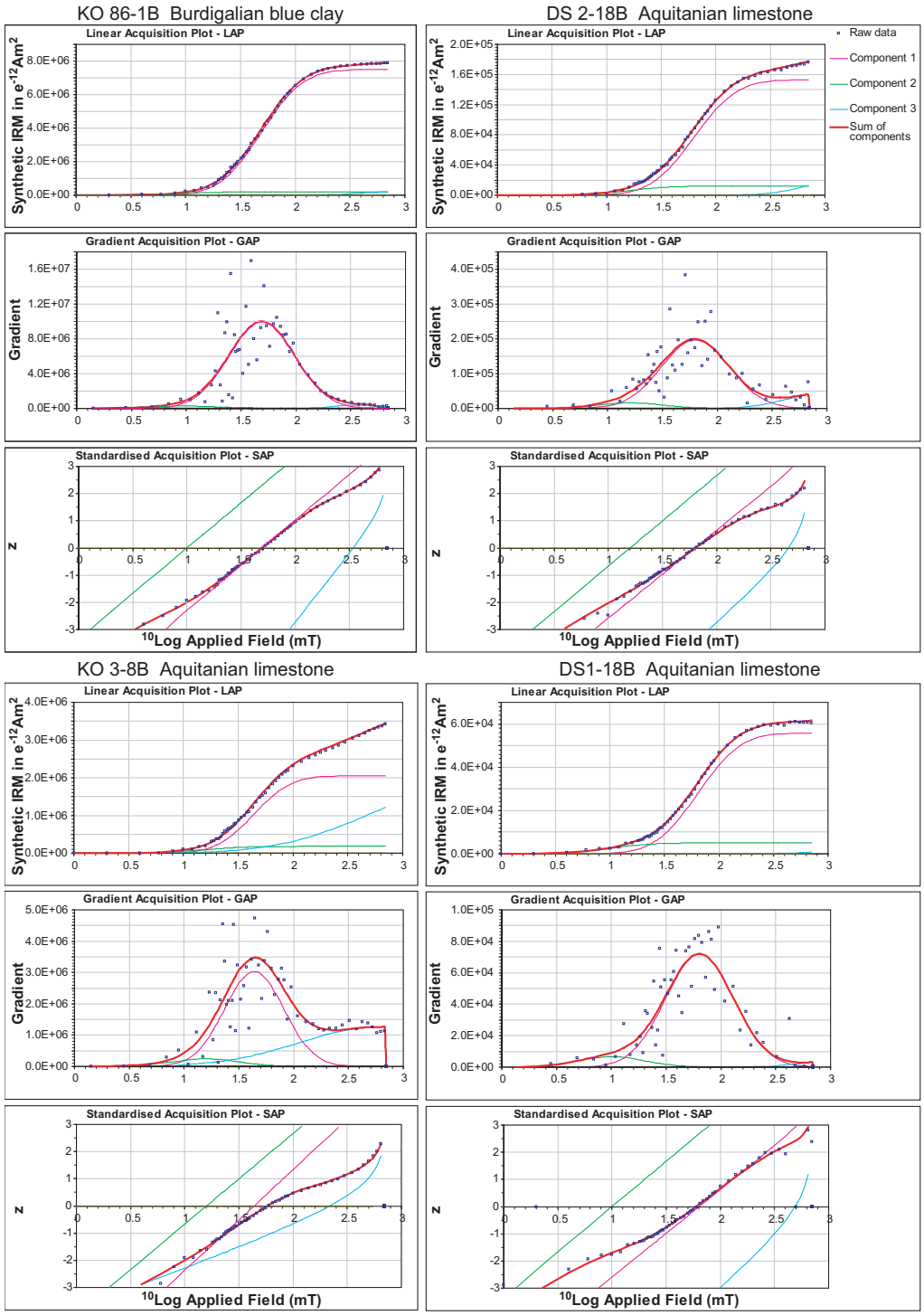

Figure 8. Examples of the interactive fitting of IRM acquisition curves (Kruiver *et al.* 2001). In most limestones component 1 (purple), interpreted to be magnetite, is harder than in the blue clays. Component 2 (green) is given no physical meaning, it is a consequence of the fitting procedure that works with symmetric distributions in the log-field space and further explanation is provided in the text. Component 3 (blue) is interpreted to be hematite. The sum of the components is given by the red curves; interactively the difference between measured data points (open squares) and the red model curve is minimized in the three representations of the data. The complete outcome of the fitting is provided in Table 2.

Table 2. Results of the IRM acquisition curve fitting (Kruiver *et al.* 2001) of all samples processed. The total saturation IRM (SIRM) is the sum of component 1 and 2 combined with the amount of component 3 added. It is based on the entire component distribution (for component 3 the measured part is only a small fraction of the total modeled component). Per component the properties are listed: %SIRM refers to the percentage of that component of the entire magnetic inventory. $logB_{1/2}$ is the remanent acquisition coercive force, $B_{1/2}$ is inverse logarithm. DP is the width of the log-Gaussian distribution (log units). $B_{1/2}$ in limestones is notably higher than in blue clays. Further explanation is given in text.

Sample	Total SIRM (Am2/kg)	Component 1				Component 3			
		% SIRM	log(B1/2) (mT)	B1/2 (mT)	DP (mT)	% SIRM	log(B1/2) (mT)	B1/2 (mT)	DP (mT)
limestones									
DS 1-6B	2.81E-06	100.0	1.85	70.8	0.32				
DS 1-9B	3.16E-06	93.1	1.81	64.6	0.29	6.9	2.70	501.2	0.30
DS 1-11B	2.45E-06	94.2	1.84	69.2	0.31	5.8	3.35	2238.7	0.35
DS 1-13B	3.03E-06	100.0	1.87	74.1	0.33				
DS 1-14B	2.42E-06	100.0	1.78	60.3	0.33				
DS 1-15A	1.19E-06	94.7	1.79	61.7	0.31	5.1	3.05	1122.0	0.30
DS 1-15B	2.45E-06	96.5	1.81	63.8	0.31	3.5	3.05	1122.0	0.30
DS 1.17B	3.49E-06	96.6	1.84	69.2	0.30	3.1	3.05	1122.0	0.30
DS 1-18B	2.77E-06	96.1	1.81	63.8	0.31	3.9	3.00	1000.0	0.30
DS 1-20A	1.85E-06	90.8	1.85	70.8	0.29	9.2	3.00	1000.0	0.30
DS 1-20B	1.60E-06	96.3	1.85	70.8	0.28	3.7	3.00	1000.0	0.30
DS 1-21B	1.70E-06	95.2	1.85	70.8	0.28	4.8	3.20	1584.9	0.30
DS 1-24B	9.70E-06	95.2	1.85	70.8	0.30	4.8	3.10	1258.9	0.30
DS 1-25B	2.00E-06	100.0	1.83	67.6	0.30				
DS 1-26B	2.01E-06	98.2	1.84	69.2	0.31	1.8	2.70	501.2	0.30
DS 1-28B	1.47E-06	97.2	1.86	74.2	0.28	2.8	3.00	1000.0	0.30
DS 1-31B	2.91E-06	96.7	1.74	55.0	0.33	3.3	3.10	1258.9	0.30
DS 1-32B	4.87E-06	59.5	1.79	61.7	0.30	40.5	3.20	1584.9	0.31
DS 1-34B	1.62E-05	26.2	1.70	50.1	0.30	73.4	3.20	1584.9	0.30
DS 1-35B	8.93E-06	30.4	1.78	60.3	0.32	69.6	3.10	1258.9	0.30
DS 2-3A	2.42E-06	84.5	1.82	66.1	0.33	15.5	3.20	1584.9	0.30
DS 2-4B	1.77E-06	93.5	1.81	64.6	0.28	6.5	2.90	794.3	0.30
DS 2-6B	2.10E-06	89.6	1.79	61.7	0.30	10.4	3.00	1000.0	0.30
DS 2-8B	4.12E-06	94.1	1.75	55.6	0.31	5.9	2.90	794.3	0.25
DS 2-15B	2.60E-06	94.9	1.81	64.6	0.31	5.1	3.00	1000.0	0.30
DS 2-16B	4.08E-06	84.9	1.79	61.7	0.30	15.1	3.10	1258.9	0.30
DS 2-18B	8.23E-06	84.6	1.80	63.1	0.31	15.4	2.90	794.3	0.30
KO 2.9B	1.99E-05	97.5	1.71	51.3	0.32	2.5	2.50	316.2	0.25
KO 2-11B	6.21E-05	93.1	1.62	41.7	0.35	6.9	2.30	199.5	0.35
KO 2-12B	3.73E-05	100.0	1.70	50.1	0.42				
KO 2-13B	7.85E-05	93.9	1.62	41.7	0.38	6.1	2.65	446.7	0.35
KO 3-6B	9.62E-05	100.0	1.77	58.9	0.34				
KO 3-7B	1.19E-04	87.4	1.63	42.7	0.33	12.6	2.60	398.1	0.38
KO 3.8B	1.96E-04	40.3	1.64	43.7	0.27	49.7	2.75	562.3	0.70
KO 3-11B	1.45E-04	79.1	1.62	41.7	0.32	20.9	2.40	251.2	0.50
KO 3-13B	6.09E-05	92.6	1.62	41.7	0.35	7.4	2.30	199.5	0.30
KO 4-2B	4.32E-04	82.7	1.52	33.1	0.31	17.3	2.60	398.1	0.37
KO 4-3B	8.17E-05	97.3	1.65	44.7	0.35	2.7	2.40	251.2	0.30
KO 5-1B	1.07E-04	97.4	1.64	43.7	0.36	2.6	2.45	281.8	0.25
KO 7-1B	2.93E-05	100.0	1.81	64.6	0.36				
KO 7-2B	8.02E-05	99.0	1.79	61.7	0.31	1.0	2.55	354.8	0.30
KO 7-3B	7.34E-05	99.2	1.79	51.7	0.32	0.8	2.55	354.8	0.30
KO 10-1B	1.45E-04	96.1	1.66	45.7	0.35	3.9	2.30	199.5	0.30
KO 10-3A	8.79E-05	98.5	1.80	63.1	0.36	1.5	2.90	794.3	0.28
blue clays									
DS 8-3A	3.46E-05	98.6	1.65	44.7	0.29	1.7	2.80	631.0	0.32
DT 7-5B	2.37E-03	98.9	1.67	46.8	0.29	1.1	3.00	1000	0.30
KO 37-1B	2.43E-04	98.3	1.69	49.0	0.29	1.7	2.50	316.2	0.20
KO 42-2B	7.80E-04	97.9	1.76	57.5	0.30	2.1	2.70	501.2	0.20
KO 52-1B	7.79E-04	94.7	1.82	66.1	0.19	5.3	2.30	199.5	0.30
KO 65-3B	1.15E-04	99.2	1.79	61.7	0.31	0.9	2.60	398.1	0.20
KO 72-3B	4.26E-04	97.9	1.65	44.7	0.30	2.1	2.65	446.7	0.24
KO 86-1B	3.09E-04	97.5	1.69	49.0	0.30	2.5	2.55	354.8	0.20

indicates single domain (SD) or small pseudo-single-domain (PSD) particles that could be partially maghemitized; this would be in line with the fairly broad DP values (which are high for detrital material). Component 3 is mathematically not well defined because only a small portion of the distribution could be measured; hence the fits are more variable with $B_{1/2}$ ranging from ~500 mT to ~2.2 Tesla. DP is around 0.30. Component 3 is probably a small fraction of hematite. In most of the section the magnetite component represents at least 95% of the magnetic inventory. Near the top of the Aquitanian limestones, the hematite proportion can be appreciable (up to ~70%), but the very weak signal precludes a clear identification in the demagnetization diagrams of this component (see below). In the two blue clay samples component 1 is distinctly softer ($B_{1/2}$ ~45 mT) than in the limestones while DP is virtually the same as in the limestones. This hints at a slightly different detrital input with larger PSD particles than those occurring in the limestone. Only a trace of Component 3 is present in the blue clays (1–2%).

In the Korkuteli section the lowermost sites (KO 2–5) show a fairly soft magnetite component 1 (average $B_{1/2}$= 44.2 mT (+50.8 / –38.4)) while higher levels have hard magnetite akin to the limestones in the Doğantaş section. Hematite percentages vary from 0 to ~4% with higher amounts of up to 50% in the KO 2–5 interval. The magnetite in the blue clays of the Korkuteli section resembles the soft magnetite in the limestones. The hematite percentage is low in the blue clays and around 2% (Table 2).

Palaeomagnetic Analysis

NRM Demagnetization – Identification of the characteristic remanent magnetization (ChRM) was done upon inspection of decay curves, equal-area projections and vector endpoint diagrams (Zijderveld 1967). The initial intensities range for the Aquitanian limestones was very low, typically from 5 to 50 μA/m, with some exceptions up to 250 μA/m. Burdigalian blue clay samples had higher initial intensities, typically between 0.5 and 4 mA/m, with some exceptions ranging up to 25 mA/m.

In most samples from Burdigalian blue clays, univectorial decay towards the origin of 90% of the NRM occurs between 15 and 70 mT and is thus defined as the ChRM (Figure 9a–e). This AF decay range is typical of magnetite or maghemite coercivities (Dunlop & Özdemir 1997). In a small fraction of the samples treated by AF demagnetization, gyroremanent magnetization (Dankers & Zijderveld 1981) occurred from ~60 mT onward and is readily identified in stereonets (Figure 9a, c). Thermal and AF demagnetization leads to similar results (Figure 9a, b). Both normal and reversed intervals could be identified (Figure 9d). Tilt-corrected samples generally show two components, one low applied field, or low temperature which resembles the present-day field, and a second rotated one. Prior to tilt correction, directions closer to, but clearly not coinciding with the present-day field were obtained (Figure 9e). The Aquitanian limestones generally gave a poor result (Figure 9f), although in some cases with slightly higher intensities sensible directions were obtained (Figure 9g).

We classified the palaeomagnetic results into three groups: The first group contains samples that provided sensible palaeomagnetic decay curves with a clear polarity and ChRM, which were used for rotation analysis (277 [81%] for Korkuteli, 38 [27%] for Doğantaş). In some cases, we could not reliably determine the declination, but the polarity was clear. These were omitted for rotation studies, but included in the magnetostratigraphic charts (48 [14%] for Korkuteli, 61 [44%] for Doğantaş). Finally, samples with behaviours such as shown in Figure 9f were discarded (15 [4%] for Korkuteli, 40 [29%] for Doğantaş).

ChRM Direction Analysis – ChRM directions were calculated by principal component analysis (Kirschvink 1980). ChRM directions with maximum angular deviation exceeding 15° were rejected from further analysis. Thus, for the Korkuteli section, 277 directions were obtained from 340 analyzed specimens. The three Doğantaş sites gave only 37 ChRM directions from 139 specimens. For each site of Doğantaş, as well as on all reversed and normal directions of both Korkuteli and Doğantaş, and finally on all normalized directions, the Vandamme (1994) cut-off was applied to discard widely outlying ChRM directions. Averages and cones of confidence

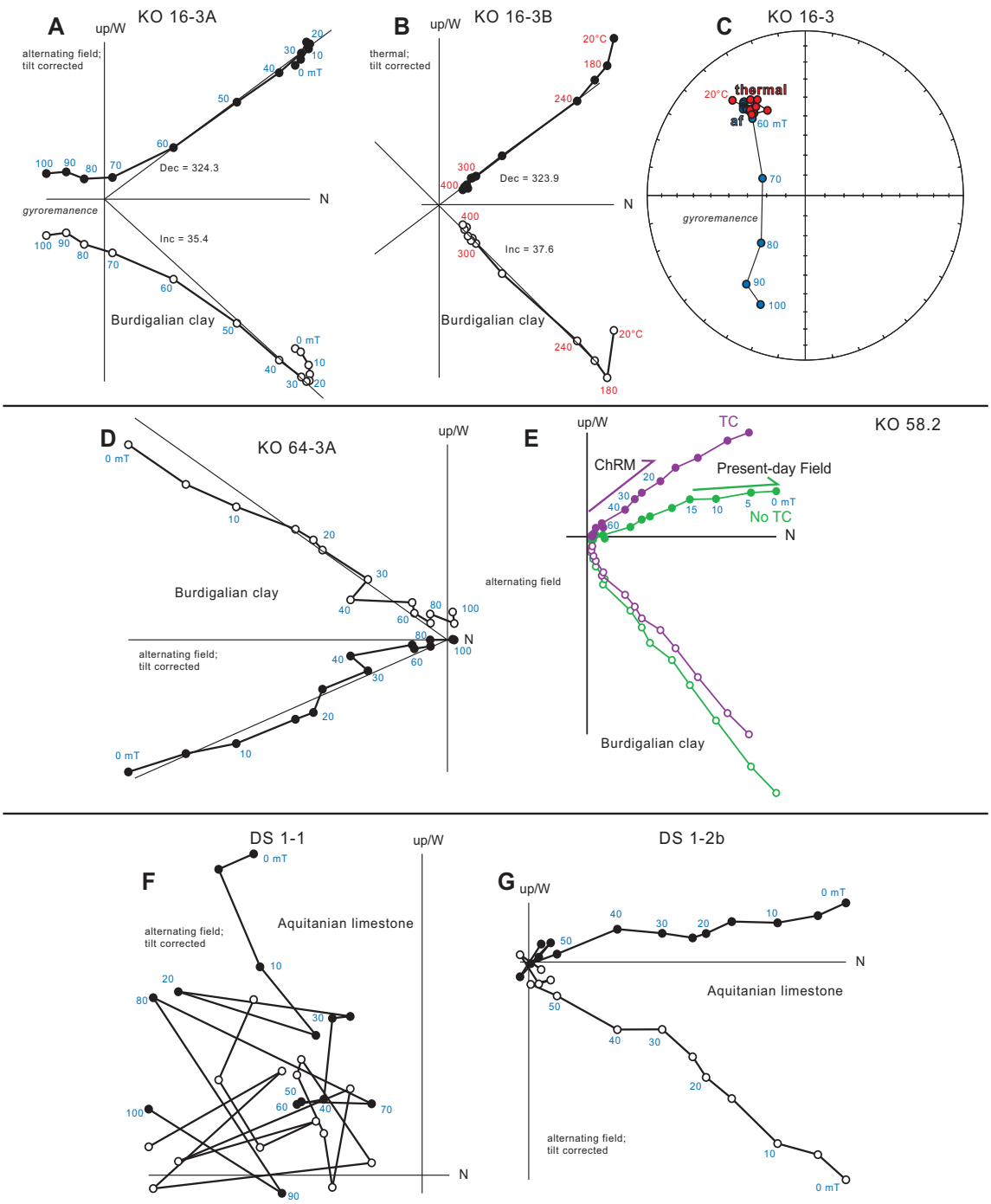

Figure 9. Typical demagnetization behaviour in Zijderveld diagrams (Zijderveld 1967) of samples from the Miocene of the Bey Dağları. **(A and B)** Reproducibility of results acquired with alternating field and thermal demagnetization, respectively. Greigite-bearing samples have a tendency to produce gyromagnetic remanence (Dankers & Zijderveld 1981), starting around 60 mT. **(C)** Stereographic projection showing the reproducibility of results using alternating field and thermal demagnetization; from 60 mT onwards, alternating field demagnetized samples start to be influenced by gyroremanence. **(D)** Typical reversed NRM; **(E)** present-day field overprints may be present and are typically removed around 15 mT. (no)TC= (not) tilt corrected; **(F)** many limestone samples, owing to very low initial intensities, provide no sensible result; **(G)** Typical Zijderveld diagram for normal magnetized Aquitanian limestones.

were determined using Fisher (1953) statistics applied on Virtual Geomagnetic Poles (VGP), because these are more Fisherian (i.e. Gaussian dispersion on a sphere) than directions, which have a (latitude dependent) elongated distribution (Tauxe & Kent 2004; Tauxe *et al.* 2008; Deenen *et al.* submitted). Errors on declination and inclination are given as ΔD_x and ΔI_x separately, following Butler (1992).

In the total average of the Korkuteli section, 16 directions were eliminated by the Vandamme (1994) cut-off, and two in the Doğantaş final average (Figure 10). Recently, Deenen *et al.* (submitted) have defined reliability criteria for palaeomagnetic data which test whether an observed distribution can be readily explained by palaeosecular variation (PSV) alone. They defined the terms $A95_{min}$ and $A95_{max}$ describing the range of A95 values for the vast majority of PSV scatters that have been reconstructed throughout earth history, and from equator to pole by e.g. McFadden *et al.* (1991) and Biggin *et al.* (2008): a VGP distribution with an A95 lower than $A95_{min}$ under-represents PSV (due for example to remagnetization, or to the sampling of sediments deposited in a very short timespan, or to averaging of PSV within sediment cores), whereas an A95 higher than $A95_{max}$ must contain an additional source of scatter, apart from PSV (e.g., rotation differences within the locality, unresolved overprints, orientation or measurement error). A95-values obtained from the Doğantaş sections and the combined locality fall within these envelopes and the data scatter from this locality therefore probably represents PSV. The Korkuteli section has A95-values slightly lower than $A95_{min}$ (Table 1). One of the potential causes for suppression of scatter is remagnetization, but in this case we do not consider this very likely. The very slight underrepresentation of PSV, probably arises because sediment samples do not represent spot readings of the Earth's magnetic field, but average out some PSV, thus decreasing the dispersion.

The A95 values of the combined, as well as the separate Doğantaş sections fall well within the reliability envelope of Deenen *et al.* (submitted); this suggests that dispersion can be explained by PSV alone. All three sections separately have A95 values lower than $A95_{max}$, and share common true mean directions (CTMDs; McFadden & Lowes 1981). The ΔD_x values of more than 10° per site still allow for small rotation differences between the sites, but the fact that the A95 value of the combined sections is still explainable by PSV alone provides us with no reason to infer significant rotation differences. Moreover, Doğantaş gives a positive reversals test of McFadden & McElhinny (1990) (Figure 10), although this reflects the large errors on the directions rather than the quality of the data.

Stratigraphical Results and Interpretation

Magnetostratigraphy

We did not specifically sample the Korkuteli section for magnetostratigraphic purposes: the main reason for sampling from bottom to top was to test whether any synsedimentary rotation occurred associated with Lycian Nappe emplacement. Yet, the obtained results can be used to see whether the measured pattern of reversals in the Korkuteli section matches the ATNTS2004 (Lourens *et al.* 2004).

The lower half of the Korkuteli section reveals a series of reversals, with short chrons. However, the large unexposed intervals, as well as the presence of mass-transported olistoplates (the largest one of which is well over 100 m thick, at around the 600 m stratigraphic level in the section; Figure 3) prohibit straightforward correlation. The top of the section, however, shows a long normal interval, followed by four well-defined reversed-normal pairs. Previous work (Poisson 1977; Gutnic *et al.* 1979; Hayward 1984b; Hayward *et al.* 1996; Karabıyıkoğlu *et al.* 2005) indicates that the age of the top of the succession in the Dariören basin is lower Langhian. Comparing our results to the timescale of Lourens *et al.* (2004) shows a straightforward match of the four reversed intervals to the upper Burdigalian, following a long normal interval. This suggests that the top of the Korkuteli section is just slightly older than ~16 Ma, in accord with published age information. The age of the bottom of the section then likely falls in the Aquitanian, also in line with published ages. Although straightforward correlation of our magnetostratigraphical information to the timescale is not possible, the large

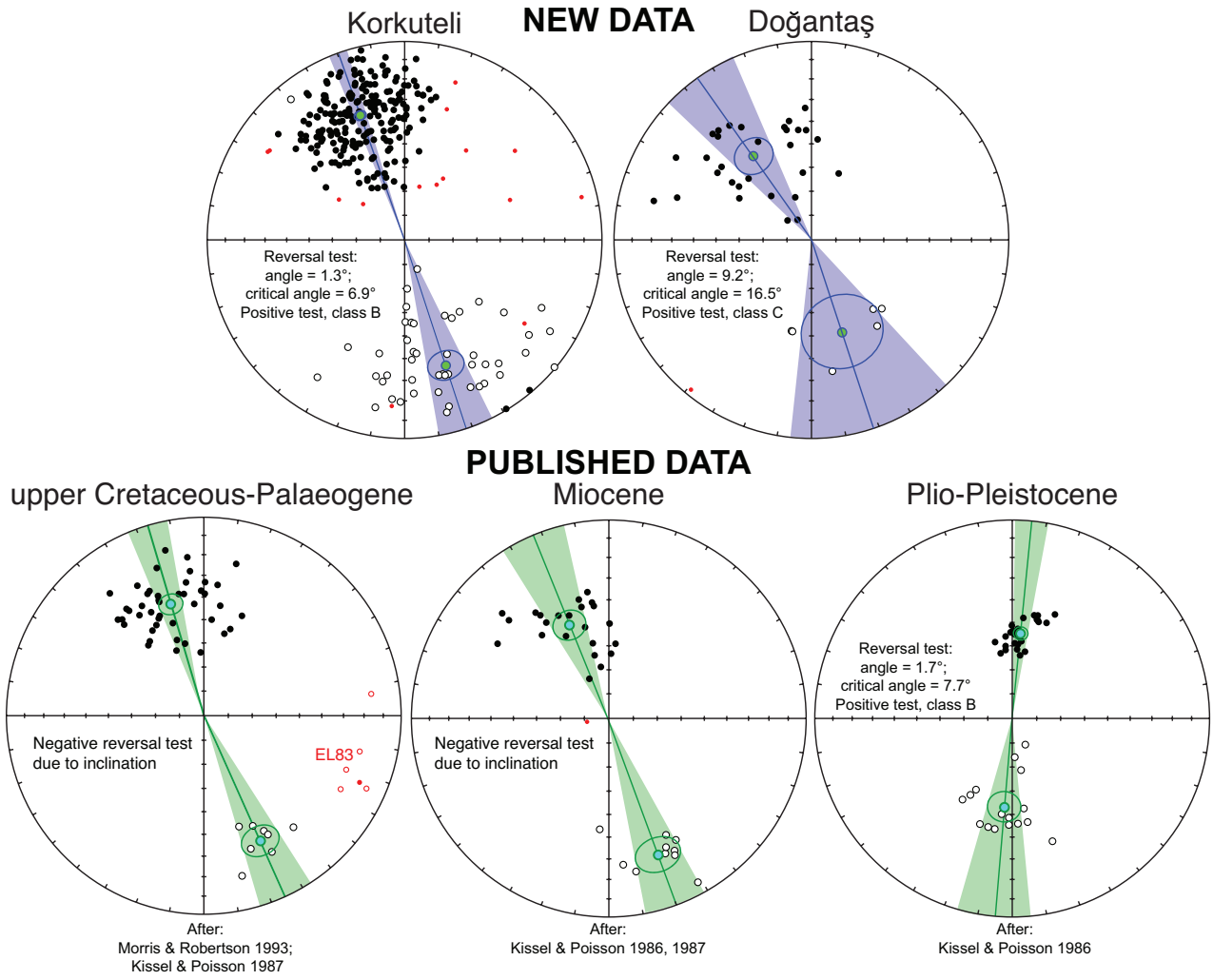

Figure 10. Upper (lower) hemisphere projections for normal (reversed) directions indicated with closed (open) circles. Reversals test results were calculated by the method of McFadden & McElhinny (1990). Red data points fell outside the Vandamme (1994) cut-off, including all data points from site EL83 of Kissel & Poisson (1987).

number and rather high frequency of reversals we obtained is not at odds with the Aquitanian polarity timescale (Figure 3).

Biostratigraphy

We analysed the planktonic foraminiferal content of several samples from the Korkuteli section (Figure 3), to confirm the published age information. The overall state of preservation, however, prevents a straightforward determination at the specific level. Even the labels assigned to the least overgrown and recrystallized specimens should be considered to be somewhat uncertain. Identifiable planktonic foraminifera in the basal samples of the section (KO 1 and 3) belong to the so-called 'large globigerinids'. This label refers to a group of large, round-chambered subbotinids, catapsydracids and globoquadrinids, which often dominates the latest Eocene to earliest Oligocene planktonic foraminiferal faunas in middle and higher latitudes (e.g., Spezzaferri 1994). The presence of specimens close to or even identical with *Turborotalia cerroazulensis* in sample KO 3 points to a latest

Eocene affinity of the planktonic foraminiferal fauna in the basal strata of the Korkuteli section. No 'large globigerinids' were observed in sample KO 9, which contains a few specimens of *Globigerinoides primordius* together with specimens close to *Globoquadrina galavisi*. The first occurrence of *Globigerinoides primordius* is recorded in the late Oligocene (Spezzaferri 1994) indicating either a large hiatus between samples KO 1-3 and KO 9 or reworking of the planktonic foraminifera at the base of the section. The reported Aquitanian ages of the basal limestones of the Miocene foreland basin (Poisson 1977; Hayward 1984c) and the presence of reworked pre-Miocene limestones in large olistoplates in the lower part of the section (Figure 4) show that the latest Eocene foraminifera are probably reworked. Rare occurrences of *Globoquadrina cf praedehiscens, Globigerinoides trilobus, Globigerinoides subquadratus, Paragloborotalia siakensis* and representatives of *Catapsydrax* in samples KO 21, 29, 85 and 86 indicate that most of the section is early Miocene. Even an earliest Miocene age for sample KO 9 cannot be excluded. The presence of a single specimen resembling *Praeorbulina sicanus* suggests that the top of the section has an age of around 16.97 Ma, corresponding with the age for the FO of the nominate species according to the ATNTS2004 (Lourens *et al.* 2004). The biostratigraphic results thus confirm the age calibration based on the magnetostratigraphy.

Discussion

Remagnetized or Primary NRM?

For the kinematic interpretation it is crucial to assess whether or not the rocks under investigation were remagnetized. This aspect has proven to be difficult and existing data are conflicting. Our data favour a primary NRM. We summarize the arguments below. Firstly, as pointed out above, the Korkuteli section has a magnetic polarity pattern that is in reasonable agreement with the lower Miocene magnetic polarity timescale for the early Miocene (Figure 3). Moreover, we obtain for both the Korkuteli section, as well as for the Doğantaş composite a positive reversals test (Figure 10) of McFadden & McElhinny (1990).

Sediments normally undergo compaction, which then also affects the palaeomagnetic field direction frozen into the sedimentary rock. If rocks become remagnetized after compaction, no evidence for flattening of the palaeomagnetic direction is expected. Both normal and reversed directions of the Korkuteli section show inclinations that are much lower than the expected value for Bey Dağları today (~56°). Therefore, we applied the elongation/inclination (E/I) method of Tauxe & Kent (2004) (Figure 11) to see whether sediment compaction had flattened the inclination and to which extent the inclination can be restored.

The E/I method was designed to correct for underestimation of the inclination in sediments as a result of compaction. The distribution of palaeomagnetic directions is not spherical but elongated, and the elongation is a function of latitude, and therefore of inclination (Tauxe & Kent 2004). Sediment compaction decreases both the elongation and the inclination (the declination normally does not change significantly), and these parameters will hence not be in accordance with each other in a palaeomagnetic dataset derived from compacted sediments. The E/I method un-flattens the dataset, until the elongation and inclination are in accordance with each other according to the statistical field model TK03 of Tauxe & Kent (2004). We applied the E/I method on the data from Korkuteli, after omitting carbonate-rich samples (to eliminate compaction differences between lithologies and magnetic mineralogies), reversed samples (in which a minor unresolved Present Day Field overprint may alter the elongation slightly), and samples that fall outside the Vandamme (1994) cut-off (to eliminate transitional directions). Unflattening the resulting dataset of n= 192 restores the inclination from 33.5° to 45.5° (Figure 11). Even though the inclination is still ~10° shallower than today (which we cannot straightforwardly geologically explain since there is no reason to assume a significant palaeolatitudinal shift of Bey Dağları since the middle Miocene), the palaeomagnetic directions of Korkuteli were flattened with a factor of 0.67. Such values are comparable to e.g. results from Crete (Krijgsman & Tauxe 2004) and Rhodes (van Hinsbergen *et al.*

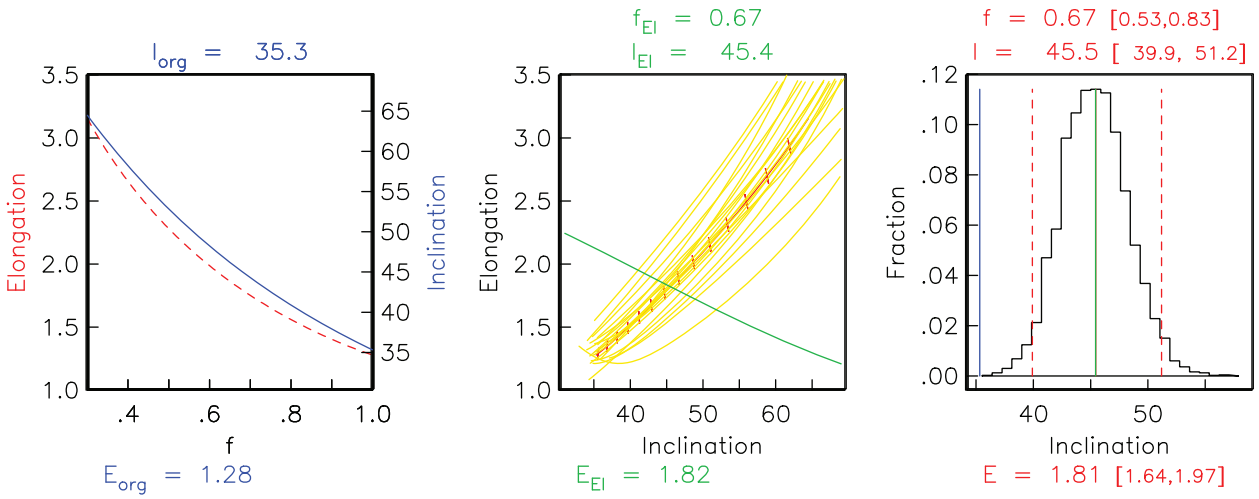

Figure 11. Plots of elongation and inclination v. flattening factor (f), as well as elongation v. inclination (thick line) for the TK03.GAD model (Tauxe & Kent 2004), for the data of the Korkuteli section, for different values of the flattening factor (f= 0.3 to 1.0). The barbs on the thick line indicate the direction of elongation of the directional distributions, with horizontal being east–west and vertical being north–south. Also shown are results from 20 boot-strapped datasets (thin dashed lines). The crossing points represent the inclination-elongation pair most consistent with the TK03.GAD model (solid thin line). The histograms represent the crossing points from 5000 boot-strapped datasets and show the most frequent inclination (vertical thick line) with 95% bounds (dashed thick lines), compared with the original inclination (vertical thin line) and the crossing points of the original distribution (thin dashed line). The corrected inclination is significantly steeper than the uncorrected one, suggesting significant compaction after acquisition of the magnetization, which is not consistent with remagnetized NRM. The corrected inclination remains, however, lower than the geocentric axial dipole (GAD) inclination (56°) for the present latitude of the Bey Dağları, which cannot be straightforwardly explained. See text for further discussion.

2007) and are in line with acquisition of the magnetization prior to compaction, for there is no reason for remagnetized directions to be flattened again. This result does not support remagnetization either.

We have carried out the fold test of Tauxe & Watson (1994) on the results from both the Korkuteli and Doğantaş sections (Figure 12). The Korkuteli section is a monoclinal succession with beds dipping northwest at between approximately 50° and 10°. The Doğantaş sections come from a monoclinal succession dipping southwest at between 5° and 30°. The fold test seeks the best clustering of a set of palaeomagnetic directions as a function of percentage of untilting. In the Doğantaş section, this is around 85% of untilting, with large error bars (95% confidence level, untilting between 58 and 104%) due to the low interlimb angle of the monoclinal succession. We consider this fold-test as positive. The result of the Korkuteli section, however, is clearer: the best clustering of palaeomagnetic data occurs at 50% untilting (Figure 12). The straightforward interpretation would be that the magnetization was acquired during folding: although this could result from remagnetization, this is not necessarily so, as the fold test determines the percentage of unfolding at which the minimum dispersion is found. However, this is not necessarily the most reliable dispersion (see also McFadden 1998). The fold test of the Korkuteli section is at odds with our other lines of evidence which do not support the case for remagnetization. Moreover, untilting the Korkuteli directions by 50%, which is still rotated CCW, and an inclination that does not resemble any expected inclination between Miocene and the Present (~55°; Torsvik *et al.* 2008). Thus, we do not interpret this negative fold test as an indication of remagnetization but attribute it to a coincidence and as a result of the low interlimb angle.

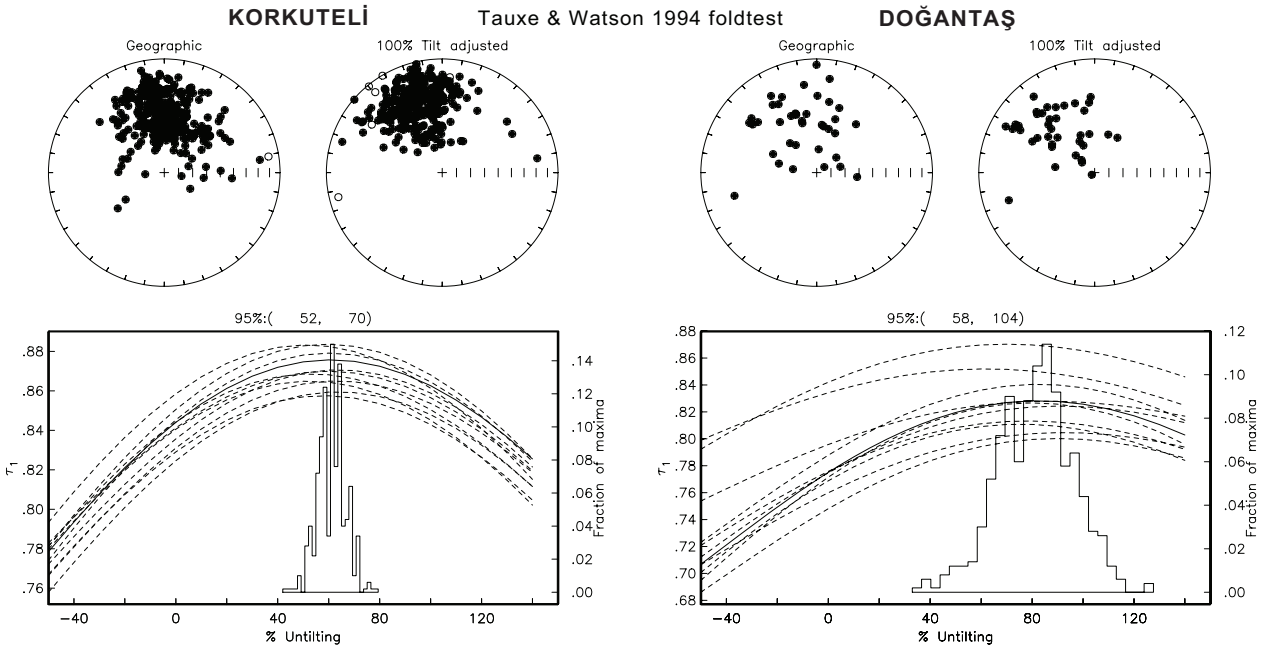

Figure 12. Fold test of Tauxe & Watson (1994) for the Korkuteli and Doğantaş localities. The dispersion in the Doğantaş data is high, and the fold test has large error bars. We consider this result a positive fold test. The fold test for the Korkuteli section is clearly negative: the best clustering of datapoints is obtained with 50% untilting. We do not consider this result conclusive for remagnetization, however. 50% unfolding does not produce a sensible direction that may have existed since deposition. Moreover, data scatter after tilt correction can still be straightforwardly explained by palaeosecular variation. See text for further discussion on this matter.

The positive reversals tests, the correlation of the magnetostratigraphy of Korkuteli to the ATNTS2004 (Lourens *et al.* 2004), and the significant flattening of the palaeomagnetic directions are all at odds with the Miocene remagnetization of the Bey Dağları as suggested by Morris & Robertson (1993). As stated above, despite being negative, the reversal test does not support remagnetization either. As yet another test for remagnetization, we carried out an end-member modelling test of IRM acquisition curves, as recently proposed by Gong *et al.* (2009).

End-member Modeling

Recently, Gong *et al.* (2009) showed the potential of end-member modelling to diagnose remagnetization in limestones from the Organyá Basin (Spain) without palaeomagnetic directional constraints. Also the study of Heslop & Dillon (2007) nicely illustrated the use of this approach to analyze and interpret subtle variations in magnetic properties in a number of geological settings. End-member modelling is based on the notion that measured data can be represented by a linear mixture of a number of invariant constituent components. These components are referred to as end-members. End-member modelling is a non-parametric technique and there is no *a priori* assumption concerning the shape of the end-members. Since the end-members are extracted from the data itself, several input curves (typically > 30) should be used to achieve a reasonable picture of the inherent data variability. The end-member modelling algorithm of Weltje (1997) is used here and programmed in MATLAB[1].

The entire IRM acquisition curve, i.e. derived from the IRM values at each field level, was used as

[1] The MATLAB modules and an executable can be found online at: http://www.marum.de/Unmixing_magnetic_remanence_curves_without_a_priori_knowledge.html

input after subtraction of background and tray contributions. Algorithm requirements dictate that input curves must be monotonic: that is the derivatives of the input data should be ≥ 0 (e.g., Heslop *et al.* 2007). Therefore the measured input IRM acquisition curves were smoothed to force them to be monotonic; this appeared to be particularly necessary at field levels < 10 mT where variable noise in the tray contribution was most prominent in comparison to a small amount of acquired IRM. Also close to saturation, in the highest field range, the difference between subsequent IRM data points can be small as well. IRM acquisition curve fits were used as a basis for smoothing. The end-member modelling program normalizes each IRM curve to its maximum value, so the input curves form a closed data set. Thus, changes in the contribution of one end-member will influence those of all other end-members. For a meaningful interpretation, the end-members must be understood and the IRM acquisition curve fits provide a firm basis for this understanding.

The program calculates the solution for a number of end-members that varies between 2 and 9. How many meaningful end-members should be considered is at the heart of the interpretation and the following criteria were used as guidelines: (1) a coefficient of determination (r^2, ranging from 0 to 1) between the input data and the end-member model (Heslop *et al.* 2007) must be > 0.8; (2) inclusion of yet another end-member provides little extra interpretational value; (3) if the extra end-member virtually duplicates an existing end-member the limit of interpretational power has been reached; (4) the program calculates the end-member model by iteration until a stopping convexity level has been reached (set at –6). A maximum 1000 iterations are performed and in the present data set the stopping criterion was never reached. Therefore the convexity level at termination was also used as judgment to assess how good the model is.

After inspection of the end-member solutions a three end-member model was selected: r^2 is 0.84 and the final convexity level is –3.8 which is reasonable. Models with a higher number of end-members have only marginally higher r^2; in contrast their convexity level is worse. From five end-member models onward, at least two of the end-members are virtually identical. For six end-member solutions the end-member shapes start to become influenced by small errors in the input data; the end-members often are often contaminated by small 'irregularities' – something which is not in line with the smooth coercivity distributions expected. In addition models with a high number of end-members gave essentially the same discrimination amongst the samples as in the three-end-member model.

The shape of the end-members is shown in Figure 13. End-member 1 is the comparatively hard SD-style magnetite typical for most limestones. End-member 2 represents the softer PSD magnetite that occurs mainly in the blue clays. Note that both saturate at 300–400 mT, in line with their anticipated non-remagnetized nature and similar to the results of Gong *et al.* (2009). The interpretation of the present end-member 3 which has a prominent low-coercivity part and a high-coercivity tail up to 700 mT is more complicated. The shape of this end-member resembles the remagnetized end-member in the study of Gong *et al.* (2009), which could imply that the samples with a high contribution of this end-member would be remagnetized, as in the data set of Gong *et al.* (2009). In the present data set, however, the hematite component happens to be unresolved as a separate end-member, unlike in the case of Gong *et al.* (2009). The hematite contribution up to 700 mT is often minute and only occasionally more prominent. Therefore the end-member algorithm (that imposes no constraints on the shape of the end-members) appears not to resolve a separate hematite end-member. To optimize the end-member interpretation we utilized the IRM acquisition curve fits: in samples where an appreciable amount of haematite was required for the fit (see Table 2), end-member 3 was considered a mixture of soft magnetite and hematite. In samples where the amount of hematite required for the IRM fit is just a few percent, a mixture of magnetite and hematite cannot be the cause for the shape of end-member 3. For these samples we invoke the possibility of remagnetization.

In the ternary plot (Figure 13), samples with high contributions to end-members 1 and 2 plot close to the base line: these are considered to carry a primary

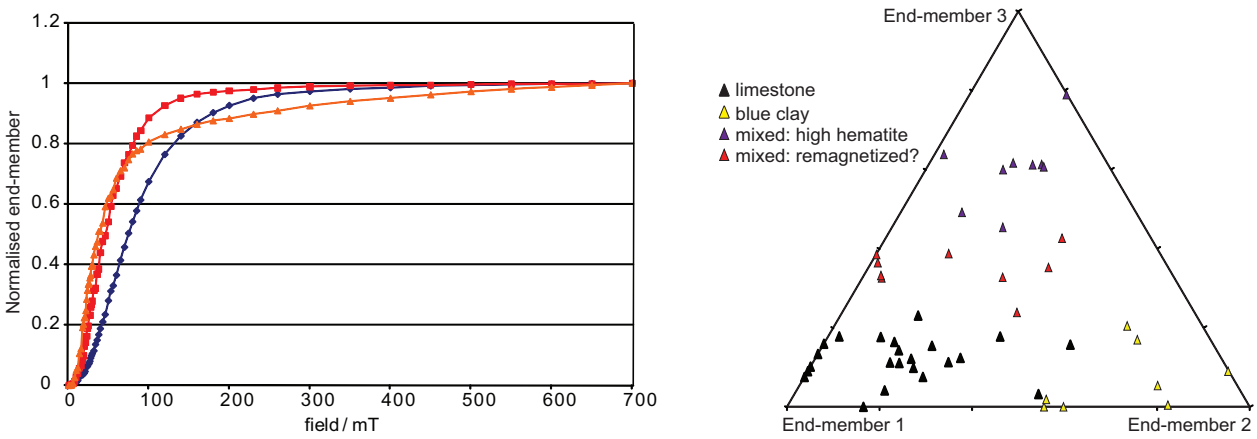

Figure 13. End-member modelling results. Left– The shape of the calculated end-members in a three-end-member model. End-member 1 (blue) is SD magnetite and occurs dominantly in the limestones. End-member 2 (red) is softer PSD magnetite and occurs mostly in the blue clays. Both saturate in 300-400 mT in line with their non-remagnetized nature (Gong *et al.* 2009). End-member 3 (orange) has a dual meaning, it represents either a mixture of magnetite and hematite (in cases where IRM acquisition curve fitting yielded a fair amount of hematite) or the samples could be remagnetized (in cases where IRM acquisition curve fitting yielded a marginal amount of hematite). Right– Ternary plot with end-member partitioning for each sample. Samples with plenty of hematite are interpreted as mixture of magnetite and hematite while samples with ~40% of end-member 3 but virtually devoid of hematite are possibly remagnetized. These all occur close to the basal unconformity. Further explanation is given in text.

NRM since the end-members saturate in 300–400 mT, in line with the shape of the magnetite end-member in the study of Gong *et al.* (2009). Limestone samples are black, blue clay samples yellow. End-member 3 has a dual interpretation: in cases where appreciable hematite was fitted to the IRM acquisition curves we label them mixture and the samples probably carry a primary NRM as well. These samples have the highest end-member 3 contribution. In those samples with raised end-member 3 contributions but with hardly any hematite required in the IRM curve fits, the possibility of remagnetization cannot be excluded. Most of those samples are in the lowest parts of the sections close to the basal unconformities, and may for instance be affected by groundwater using the unconformity as aquifer. Note that this is only a very small fraction of the total amount of samples. The vast majority of the samples (>95%) which determine the rotation and magnetic polarity of the sections were taken from blue clay, which provides no reason at all to suspect remagnetization.

The end-member analysis concurs with our earlier inferences: regional, widespread remagnetization in the Miocene history of Bey Dağları (in the Dariören and Kasaba sub-basins), such as that suggested by Morris & Robertson (1993) is not likely.

Re-evaluation of Previous Arguments for Remagnetization

In their thought-provoking and interesting work, Morris & Robertson (1993) reported results from 12 sites in three geological domains: five sites from upper Cretaceous to Eocene carbonates in the Bey Dağları (YA, CD, FI, DA and DK), three sites from carbonate units in Tauride thrust sheets and four sites from the Antalya Nappes (Figure 2). They argued that these sites were pervasively remagnetized and postulated fluid migration as a cause of the remagnetization which would be a chemical remanent magnetization (CRM).

Because the present data do not support this view, we re-examine the evidence for this conclusion. Morris & Robertson (1993) argued that the five sites in the Bey Dağları are remagnetized, based on a negative fold test between their sites YA and FI. First we note that these two sites that are approximately 50 km apart. The negative fold test may therefore well

be the result of anomalous behaviour of one of these sites. Further, we calculate whether the five sites from the Bey Dağları (Morris & Robertson 1993) share common true mean directions following McFadden & Lowes (1981) prior to and after tilt correction, based on the published statistical values. The result shows that that sites FI, CA, DA and DK share a post-tilt correction CTMD, but none shared a CTMD prior to tilt correction (with the exception of FI and CD, which both before and after tilt correction shared a CTMD). We cannot carry out a proper fold test, because the bedding orientation of these sites was not published, but the CTMD test on the 0% and 100% tilt-corrected values strongly suggest a positive fold test. The argument for remagnetization of the Bey Dağları thus seems to rely heavily on the deviant site YA. The anomalous behaviour of site YA may result from remagnetization indeed: although debate exists as to how far the Antalya Nappes have travelled, there is general consensus that they came from the north (Marcoux *et al.* 1989; Poisson *et al.* 2003b) and if so, the Antalya Nappes could have overthrust and remagnetized site YA. The other sites may not have been reached by the nappe stack and the published data give no reason to suspect remagnetization.

Hence, we conclude that evidence for widespread remagnetization of the Bey Dağları carbonates is relatively meagre. Indeed, Morris & Robertson (1993) acknowledge that the sites of Maastrichtian to Miocene age sampled by Lauer (1981) and Kissel & Poisson (1987) in the Bey Dağları carbonate platform may retain primary depositional remanences because these sites record both normal and reversed polarities.

It is beyond the scope of this paper to assess the remagnetization in the Taurides and Antalya Nappes in detail. Morris & Robertson (1993) provided compelling evidence that at least part of the Antalya Nappes underwent remagnetization because palaeomagnetic directions from this region show a comparable orientation to those from the Bey Dağları and *in situ* fold tests within a single locality are negative. Other authors (Gallet *et al.* 1993, 1996, 2000) on the other hand, published seemingly reliable Triassic magnetostratigraphies from sections in the Antalya Nappes and the Taurides which contradict pervasive remagnetization. Hence, results are inconclusive and future analysis is required. Our new data, along with a re-examination of published information, however, exclude regional, widespread remagnetization of the Bey Dağları carbonate platform or the overlying foreland basin deposits, either in the Miocene, or since the late Cretaceous.

Timing and Amount of Rotation in Southwestern Turkey

It is timely to re-evaluate the timing and amount of rotation of the Bey Dağları. Because they concluded that remagnetization occurred throughout the Bey Dağları, Morris & Robertson (1993) chose not to correct for bedding tilt in their calculation of the amount of rotation. Using their tilt-corrected values (omitting site YA of Morris & Robertson 1993) for reasons outlined in the previous section, and site EL83 of Kissel & Poisson (1987), which is eliminated by the Vandamme (1994) cut-off, our compiled Cretaceous to Eocene palaeomagnetic direction (Figure 10) gives a $D\pm\Delta D_x/I\pm\Delta I_x$ of 341.9±4.6°/39.5±5.9° (Table 1), which shows a 20° CCW rotation, somewhat smaller than rotations inferred by Kissel & Poisson (1987) and Morris & Robertson (1993).

The declination of the Korkuteli section agrees well with the declination of the Miocene sites of Kissel & Poisson (1986, 1987; Table 1): 340.4±5.7° versus 338.0±6.2°. The declination of the Doğantaş composite confirms a CCW rotation of the Bey Dağları of 327.8±9.0°. This somewhat higher rotation may be the result of local rotations having added to the regional rotation, e.g., due to deformation related to the Susuzdağ thrust, but the lower data quality (note the larger error bar) does not allow any firm conclusions to be drawn.

The Bey Dağları platform probably formed part of the underriding African plate until the Eocene collision of its northern promontory with overriding plate in the Eocene (Şengör & Yılmaz 1981; Collins & Robertson 1998; Bozkurt & Oberhänsli 2001). Expected declinations for the Bey Dağları based on the African apparent polar wander path of Torsvik *et al.* (2008) between 70 and 60 Ma are 359° to 2°, i.e. essentially north. The consistent declinations

throughout the Bey Dağları stratigraphy show that there has been no rotation of this region between the late Cretaceous and the early Miocene times.

Moreover, the fact that the dispersion of palaeomagnetic directions in especially the Korkuteli section, spanning the Aquitanian to uppermost Burdigalian (Figure 3) can be straightforwardly explained by PSV alone shows that there has been no significant rotation during deposition of the sampled stratigraphy. The ~20° CCW rotation of Bey Dağları therefore postdates the early Miocene.

Finally, the data from the Antalya Nappes (Morris & Robertson 1993) suggest that all their sites (Figure 2) were part of the rotating domain, as were the sites at the eastern end of the Bey Dağları region sampled by these authors, which also seem to have experienced the Bey Dağları rotation. The Plio–Pleistocene sites of Kissel & Poisson (1986), sampled in the heart of the Isparta Angle are therefore sampled within the rotating domain. Although the A95s of five of their sites fall below the $A95_{min}$, suggesting under-representation of PSV, a positive reversals test after McFadden & McElhinny (1990) that we calculated from their data (Figure 10) makes us confident that our combined direction of 5.8°±4.1°/53.3±3.5° is reasonable. This confines the timing of the counterclockwise rotation phase of Bey Dağları to middle–late Miocene, i.e. sometime between 16 and 5 Ma. A Pleistocene 25° CCW rotation phase of Rhodes (van Hinsbergen *et al.* 2007; see Figure 2) is thus clearly younger and unrelated to the rotation of the Bey Dağları.

Tectonic Accommodation of the Rotations

Combining our results with previously published geological information on western Turkey may allow us to identify the structures that accommodated this rotation of SW Turkey. To the south, the free edge formed by the plate boundary with Africa was the likely accommodator. In the east, the age of the rotation phase coincides with the evolution of the Köprü and Aksu basins, and movement of their bounding strike-slip and thrust faults, respectively (Poisson 1977; Flecker *et al.* 1995, 1998; Poisson *et al.* 2003a). Previous researchers have related the E–W compression creating the Aksu fault to the westward escape of Anatolia in the late Miocene (McKenzie 1978; Dumont *et al.* 1979; Şengör & Yılmaz 1981), but we consider it more likely that the Aksu and Kırkkavak faults are partitioning strain induced by the Bey Dağları rotation into a thrust fault and dextral strike-slip fault, respectively (Figure 14), a phenomenon well-known from transpressional strike-slip belts (Cunningham 2005, 2007).

The Lycian Nappes were emplaced over the northwestern limit of the Bey Dağları and created the foreland with the stratigraphy sampled in this study (Hayward & Robertson 1982; Hayward 1984b; Collins & Robertson 1997). The end of the emplacement can be dated by the youngest sediments below the thrust (see also van Hinsbergen *et al.* 2005c; Hüsing *et al.* 2009) as early Langhian. Our new data thus show that the Lycian Nappes were emplaced prior to the rotation of the Bey Dağları and the thrust in between these units hence did not accommodate the rotation (Figure 14). The accommodation of the rotation in the northwest must thus be located within or north of the Lycian Nappes, such as for instance in the Menderes Massif, where large-scale middle to late Miocene extension has been accommodated (Hetzel *et al.* 1995b; Bozkurt 2001; Gessner *et al.* 2001; Işık *et al.* 2003). Testing this interpretation requires determination of the location of the rotation pole for the SW Turkish rotations, and new palaeomagnetic data from western Turkey. This forms the subject of an another paper (van Hinsbergen *et al.* 2010).

Finally, Platzman *et al.* (1998) and Kissel *et al.* (2003) published and compiled palaeomagnetic data from central and eastern Anatolia, and averaged these to conclude a 20–30° counterclockwise rotation for the entire Anatolian block in the Miocene. If this is correct, the rotation of the Bey Dağları, which was not included in this average, would not be related to SW Anatolian tectonics, but rather formed part of this Anatolian rotation. These compilation studies, however, did not take into account the possibility of more local central and east Anatolian rotations, e.g. resulting from widespread strike-slip deformation (Şengör *et al.* 1985), and sustaining these inferences will require a more thorough analysis. The presence of structures in western Turkey that may account for a rotation phase restricted to SW Turkey leads us to

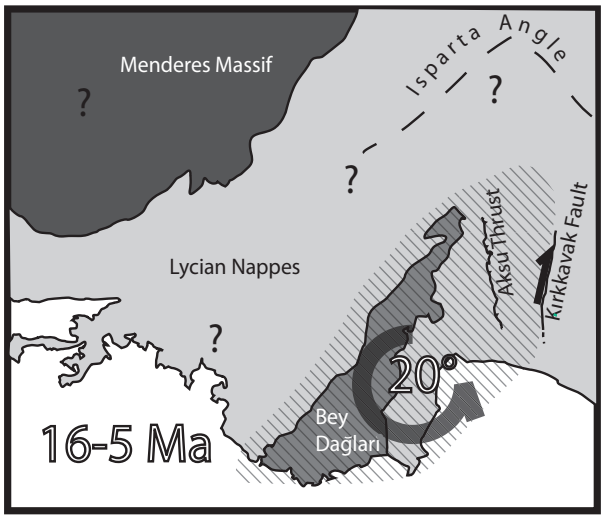

Figure 14. Summary of our new findings: rotation of the Bey Dağları occurred over 20° counterclockwise between 16 and 5 Ma ago. It was probably accommodated in the east by right-lateral transpressional shear partitioned over the Kırkkavak dextral strike-slip fault and the Aksu thrust. To date, it is unknown how the rotation of Bey Dağları is kinematically accommodated in the north and west, but we conclude that this is likely within or north of the Lycian Nappes: the thrust below the Lycian Nappes predates the rotations and probably played no role in their accommodation.

infer – at least at this stage – that this region forms the eastern limb of the Aegean orocline, and rotated within the same time span – 16 to 5 Ma – as the western limb, which was rotated largely between 15 and 8 Ma (van Hinsbergen *et al.* 2005b).

Conclusions

Southwestern Anatolia hosts the eastern limb of the Aegean orocline. The Bey Dağları region in SW Turkey, exposing upper Cretaceous to Eocene platform carbonates and lower Miocene flysch deposits, was previously been reported to have rotated 25–30° CCW following a Miocene remagnetization event. Here, we evaluate these previous inferences by sampling two (composite) sections near Korkuteli and Doğantaş. These contain lower Miocene foreland basin deposits, from an Aquitanian unconformity with the Bey Dağları limestones, to the uppermost Burdigalian to lowermost Langhian. We carried out a broad array of palaeomagnetic analyses on these samples, which allowed us to conclude that:

1. The NRM in Aquitanian limestones and Burdigalian blue clays is dominantly carried by magnetite, with minor greigite and hematite.
2. Both sections provide a positive reversals test. The upper half of the Korkuteli section can be confidently correlated to the geomagnetic polarity timescale; the lower part is not at odds with it. The Korkuteli section underwent significant compaction following acquisition of the magnetization. Palaeomagnetic directions from both sections can be straightforwardly explained by palaeosecular variation; The Doğantaş section provides a positive fold test; section Korkuteli section provides a negative fold test but we think it unlikely that this results from syn-folding remagnetization.
3. Our data indicate a primary NRM and that widespread Miocene remagnetization of the Bey Dağları is highly unlikely. A recently proposed IRM end-member model test confirms this conclusion.
4. Reassessment of the published arguments recognizes no need to assume an upper Cretaceous to Eocene remagnetization of the Bey Dağları.
5. Miocene declinations are comparable to published late Cretaceous to Eocene ones and the Bey Dağları evidently underwent no rotation between the late Cretaceous and late Burdigalian.
6. The Bey Dağları underwent 20° CCW rotation in the middle to late Miocene, i.e. between ~16 and 5 Ma, prior to deposition of previously-reported non-rotated Pliocene sediments north of Antalya.
7. The two limbs of the Aegean orocline rotated within the same time span: 16–5 Ma in the east versus (largely) 15–8 Ma in the west.
8. The rotation of the Bey Dağları was probably bounded in the south by the plate boundary with Africa, and in the east by the Aksu thrust and Kırkkavak right-lateral strike-slip fault, which partitioned dextral transpression induced by the rotating block. The northern and western accommodation will require future work.

Acknowledgements

Jan-Willem Zachariasse's help with the biostratigraphic elements of this paper is greatly appreciated. We thank Annemiek Asschert and Erhan Gülyüz for their help in the field. Nuretdin Kaymakcı is thanked for discussion, logistical support, and Turkish translation of the abstract. We appreciate reviews by John Piper and Aral Okay and editorial comments of Erdin Bozkurt. Marijn Koopman is thanked for thermally demagnetizing a set of Bey Dağları samples. The Netherlands Science Foundation (NWO) is acknowledged for funding the robotized magnetometer we used in this study. DJJvH was supported by an NWO VENI grant and acknowledges financial support from Statoil (SPlates Model). English of the final text is edited by John A Winchester.

References

Akay, E. & Uysal, S. 1981. *Orta Torosların Batısındaki (Antalya) Neojen Çökellerinin Stratigrafisi, Sedimentolojisi ve Yapısal Jeolojisi [Stratigraphy, Sedimentology and Structural Geology of Neogene Sediments in the West of Central Taurides (Antalya)]*. Mineral Research and Exploration Institute (MTA) Turkey Report no. **276** [unpublished, in Turkish].

Akay, E., Uysal, S., Poisson, A., Cravette, J. & Müller, C. 1985. Antalya Neojen havzasının straigrafisi [Stratigraphy of Antalya Neogene Basin]. *Bulletin of the Geological Society of Turkey* **28**, 105–119.

Alçiçek, M.C. 2007. Tectonic development of an orogen-top rift recorded by its terrestrial sedimentation pattern: The Neogene Esen Basin of southwestern Anatolia. *Sedimentary Geology* **200**, 117–140.

Aubouin, J. 1957. Essai de corrélation stratigraphique de la Grèce occidentale. *Bulletin de la Societe Geologique de France* **7**, 281–304.

Bağci, U. & Parlak, O. 2009. Petrology of the Tekirova (Antalya) ophiolite (Southern Turkey): evidence for diverse magma generations and their tectonic implications during Neotethyan-subduction. *International Journal of Earth Sciences* **98**, 387–405.

Barka, A. & Reilinger, R. 1997. Active tectonics of the Eastern Mediterranean region: deduced from GPS, neotectonic and seismicity data. *Annali di Geofisica* **40**, 587–610.

Beck, M.E., Burmester, R.F., Kondopoulou, D.P. & Atzemoglou, A. 2001. The palaeomagnetism of Lesbos, NE Aegean, and the eastern Mediterranean inclination anomaly. *Geophysical Journal International* **145**, 233–245.

Bernoulli, D., DeGraciansky, P.C. & Monod, O. 1974. The extension of the Lycian Nappes (SW Turkey) into the SE Aegean islands. *Eclogae Geologicae Helveticae* **67**, 39–90.

Biggin, A., van Hinsbergen, D.J.J., Langereis, C.G., Straathof, G.B. & Deenen, M.H. 2008. Geomagnetic Secular variation in the Cretaceous Normal Superchron and in the Jurassic. *Physics of the Earth and Planetary Interiors* **169**, 3–19.

Bizon, G., Biju-Duval, B., Letouzay, J., Monod, O., Poisson, A., Özer, B. & Öztümer, E. 1974. Nouvelles précisions stratigraphiques concernant les bassins tertiaires du sud de la Turquie (Antalya, Mut, Adana). *Revue de l'Institut Français du Pétrol, Paris* **29**, 305–320.

Blumenthal, M.M. 1963. Le système structural du Taurus sud Anatolies. Bulletin de la Société Géologique de France. *Livre à Mémoire de Professor P. Fallot, Mémoir hors-série* **1**, 611–662.

Bozkurt, E. 2001. Late Alpine evolution of the central Menderes Massif, western Turkey. *International Journal of Earth Sciences* **89**, 728–744.

Bozkurt, E. 2004. Granitoid rocks of the southern Menderes Massif (southwestern Turkey): field evidence for Tertiary magmatism in an extensional shear zone. *International Journal of Earth Sciences* **93**, 52–71.

Bozkurt, E. 2007. Extensional v. contractional origin for the southern Menderes shear zone, SW Turkey: tectonic and metamorphic implications. *Geological Magazine* **144**, 191–210.

Bozkurt, E. & Oberhänsli, R. 2001. Menderes Massif (Western Turkey): structural, metamorphic and magmatic evolution - a synthesis. *International Journal of Earth Sciences* **89**, 679–708.

Bozkurt, E. & Park, R.G. 1994. Southern Menderes Massif: an incipient metamorphic core complex in western Anatolia, Turkey. *Journal of the Geological Society, London* **151**, 213–216.

Bozkurt, E. & Satir, M. 2000. The southern Menderes Massif (western Turkey): geochronology and exhumation history. *Geological Journal* **35**, 285–296.

Brunn, J.H., De Graciansky, P.C., Gutnic, M., Juteau, T., Lefévre, R., Harcoux, J., Monod, O. & Poisson, A. 1970. Structures majeurs et correlations stratigraphiques dans les Taurides occidentales. *Bulletin de la Société Géologique de France* **12**, 515–551.

Butler, R.F. 1992. *Palaeomagnetism: Magnetic Domains to Geologic Terranes*: Boston, Blackwell Scientific Publications.

Candan, O., Dora, Ö.O., Oberhänsli, R., Çetinkaplan, M., Partzsch, J.H., Warkus, F.C. & Dürr, S. 2001. Pan-African high-pressure metamorphism in the Precambrian basement of the Menderes Massif, Western Anatolia, Turkey. *International Journal of Earth Sciences* **89**, 793–811.

Carey, S.W. 1958. A tectonic approach to continental drift. *In* Carey, S.W., (ed), *Continental Drift- A Symposium, Hobart, Tasmania*, 177–355.

Çelik, Ö.F. 2008. Detailed geochemistry and K-Ar geochronology of the metamorphic sole rocks and their mafic dykes from the Mersin Ophiolite, Southern Turkey. *Turkish Journal of Earth Sciences* **17**, 685–708.

Çelik, Ö.F., Delaloyle, M.F. & Feraud, G. 2006. Precise ^{40}Ar-^{39}Ar ages from the metamorphic sole rocks of the Tauride Belt Ophiolites, southern Turkey: implications for the rapid cooling history. *Geological Magazine* **143**, 213–227.

Cihan, M., Saraç, G. & Gökçe, O. 2003. Insights into biaxial extensional tectonics: an example from the Sandıklı Graben, western Anatolia, Turkey. *Geological Journal* **38**, 47–66.

Çiner, A., Karabiyikoğlu, M., Monod, O., Deynoux, M. & Tuzcu, S. 2008. Late Cenozoic sedimentary evolution of the Antalya Basin, Southern Turkey. *Turkish Journal of Earth Sciences*, **17**, 1–41.

Collins, A.S. & Robertson, A.H.F. 1997. Lycian melange, southwestern Turkey: an emplaced Late Cretaceous accretionary complex. *Geology* **25**, 255–258.

Collins, A.S. & Robertson, A.H.F. 1998. Processes of Late Cretaceous to Late Miocene episodic thrust-sheet translation in the Lycian Taurides, SW Turkey. *Journal of the Geological Society, London* **155**, 759–772.

Collins, A.S. & Robertson, A.H.F. 2003. Kinematic evidence for Late Mesozoic–Miocene emplacement of the Lycian allochthon over the Western Anatolide Belt, SW Turkey. *Geological Journal* **38**, 295–310.

Cunningham, W.D. 2005. Active intracontinental transpressional mountain building in the Mongolian Altai: defining a new class of orogen. *Earth and Planetary Science Letters* **240**, 436–444.

Cunningham, W.D. 2007. Structural and topographic characteristics of restraining bend mountain ranges of the Altai, Gobi Altai and easternmost Tien Shan. *In:* Cunningham, W.D. & Mann, P. (eds), *Tectonics of Strike-slip Restraining and Releasing Bends*. Geological Society, London, Special Publications **290**, 219–237.

Dankers, P.H.M. & Zijderveld, J.D.A. 1981. Alternating field demagnetization of rocks, and the problem of gyromagnetic remanence. *Earth and Planetary Science Letters* **53**, 89–92.

De Graciansky, P.C. 1972. *Recherches géologiques dans le Taurus lycien occidental*. Thèse Doctorat d'État, Université Paris Sud (Orsay).

Deenen, M.H.L, Langereis, C.G., van Hinsbergen, D.J.J. & Biggin, A.J. Submitted. Geomagnetic secular variation and the statistics of palaeomagnetic directions. *Geophysical Journal International*.

Deynoux, M., Çiner, A., Monod, O., Karabiyikoğlu, M., Manatschal, G. & Tuzcu, S. 2005. Facies architecture and depositional evolution of alluvial fan to fan-delta complexes in the tectonically active Miocene Köprüçay Basin, Isparta Angle, Turkey. *Sedimentary Geology* **173**, 315–343.

Dilek, Y. & Whitney, D.L. 1997. Counterclockwise P-T-t trajectory from the metamorphic sole of a Neo-Tethyan ophiolite (Turkey). *Tectonophysics* **280**, 295–310.

Duermeijer, C.E., Krijgsman, W., Langereis, C.G. & ten Veen, J.H. 1998. Post early Messinian counter-clockwise rotations on Crete: implications for the late Miocene to Recent kinematics of the southern Hellenic Arc. *Tectonophysics* **298**, 77–89.

Dumont, J.F., Gutnic, M., Marcoux, J., Monod, O. & Poisson, A. 1972. Le Trias des Taurides occidentales (Turquie). Definition du bassin pamphylien: un nouveau domain à ophiolites à la marge externe de la chaine taurique. *Zeitschift Deutsche Geologische Gesellschaft* **123**, 385–409.

Dumont, J.F. & Kerey, E. 1975. L'accident de Kirkkavak, un decrochement majeur dans le Taurus occidental (Turquie). *Bulletin de la Société Géologique de France* **7**, 1071–1073.

Dumont, J.F., Poisson, A. & Şahinci, A. 1979. Sur l'existence de coulissements sinistres recentes a l'extermité orientale de l'arc ageen (sud-ouest de la Turquie). *Comptes Rendus Acadademie Science Paris* **289**, 261–264.

Dunlop, D. & Özdemir, Ö. 1997. *Rock Magnetism: Fundamentals and Frontiers*: Cambridge, Cambridge University Press.

Egli, R. 2003. Analysis of the field dependence of remanent magnetization curves. *Journal of Geophysical Research* **108**, 2081, doi:10,1029/2002JB002023.

Egli, R. 2004. Characterization of individual rock magnetic components by analysis of remanence curves. 2. Fundamental properties of coercivity distributions. *Physics and Chemistry of the Earth* **29**, 851–867.

Farinacci, A. & Köylüoğlu, M. 1982. Evolution of the Jurassic–Cretaceous Taurus shelf (southern Turkey). *Boletino della Società Palaeontologica Italiana* **21**, 267–276.

Fisher, R.A. 1953. Dispersion on a sphere. *Proceedings of the Royal Society of London* **A217**, 295–305.

Flecker, R., Ellam, R.M., Müller, C., Poisson, A., Robertson, A.H.F. & Turner, J. 1998. Application of Sr isotope stratigraphy and sedimentary analysis to the origin and evolution of the Neogene basins in the Isparta Angle, southern Turkey. *Tectonophysics* **298**, 83–101.

Flecker, R., Poisson, A. & Robertson, A.H.F. 2005. Facies and palaeogeographic evidence for the Miocene evolution of the Isparta Angle in its regional eastern Mediterranean context. *Sedimentary Geology* **173**, 277–314.

Flecker, R.M., Robertson, A.H.F., Poisson, A. & Müller, C. 1995. Facies and tectonic significance of two contrasting Miocene basins in south coastal Turkey. *Terra Nova* **7**, 221–232.

Forster, M.A. & Lister, G.S. 2009. Core-complex-related extension of the Aegean lithosphere initiated at the Eocene–Oligocene transition. *Journal of Geophysical Research* **114**, B02401, doi:10.1029/2007JB005382.

Frizon de Lamotte, D., Poisson, A., Aubourg, C. & Temiz, H. 1995. Chevauchements post Tortoniens vers L'ouest puis vers le sud au coeur de l'Angle d'Isparta (Taurus, Turquie). Conséquences Géodynamiques. *Bulletin de la Société Géologique de France* **166**, 57–66.

Gallet, Y., Besse, J., Krystyn, L. & Marcoux, J. 1996. Norian magnetostratigraphy from the Scheiblkogel section, Austria: constraint on the origin of the Antalya Nappes, Turkey. *Earth and Planetary Science Letters* **140**, 113–122.

Gallet, Y., Besse, J., Krystyn, L., Marcoux, J., Guex, J. & Théveniaut, H. 2000. Magnetostratigraphy of the Kavaalanı section (southwestern Turkey): consequence for the origin of the Antalya Calcareous Nappes (Turkey) and for the Norian (Late Triassic) magnetic polarity timescale. *Geophysical Research Letters* **27**, 2033–2036.

Gallet, Y., Besse, J., Krystyn, L., Theveniaut, H. & Marcoux, J. 1993. Magnetostratigraphy of the Kavur Tepe section (southwestern Turkey): a magnetic polarity timescale for the Norian. *Earth and Planetary Science Letters* **117**, 443–456.

Gessner, K., Ring, U., Johnson, C., Hetzel, R., Passchier, C.W. & Güngör, T. 2001. An active bivergent rolling-hinge detachment system: Central Menderes metamorphic core complex in western Turkey. *Geology* **29**, 611–614.

Glover, C.P. & Robertson, A.H.F. 1998a. Neotectonic intersection of the Aegean and Cyprus tectonic arcs: extensional and strike-slip faulting in the Isparta Angle, SW Turkey. *Tectonophysics* **298**, 103–132.

Glover, C.P. & Robertson, A.H.F. 1998b. Role of regional extension and uplift in the Plio–Pleistocene evolution of the Aksu Basin, SW Turkey. *Journal of the Geological Society, London* **155**, 365–387.

Glover, C.P. & Robertson, A.H.F. 2003. Origin of tufa (cool-water carbonate) and related terraces in the Antalya area, SW Turkey. *Geological Journal* **38**, 329–358.

Gong, Z., Dekkers, M.J., Heslop, D. & Mullender, T.A.T. 2009. End-member modeling of isothermal remanent magnetization (IRM) acquisition curves: a novel approach to diagnose remagnetization. *Geophysical Journal International* **178**, 693–701.

Gutnic, M., Monod, O., Poisson, A. & Dumont, J.F. 1979. Géologie des Taurides occidentales (Türquie). *Mémoir de Société Géologique de France* **137**, 1–112.

Hayward, A.B. 1983. Coastal alluvial fans of Miocene age in S.W. Turkey. *In*: Collinson, J.D. & Lewin, J., (eds), *Modern and Ancient Fluvial Systems. Sedimentology Special Publications* **6**, 323–336.

Hayward, A.B. 1984a. Hemipelagic chalks in a clastic submarine fan sequence. *In:* Stow, D.A.V. & Piper, D.J.W. (eds), *Fine-grained Sediments.* Geological Society, London, Special Publications **14**, 453–467.

Hayward, A.B. 1984b. Miocene clastic sedimentation related to the emplacement of the Lycian Nappes and the Antalya Compex, S.W. Turkey. *In:* Dixon, J.E. & Robertson, A.H.F. (eds), *Geological Evolution of the Eastern Mediterranean.* Geological Society, London Special Publications **17**, 287–300.

Hayward, A.B. 1984c. Sedimentation and basin formation related to ophiolite nappe emplacement, Miocene, SW Turkey. *Sedimentary Geology* **71**, 105–129.

Hayward, A.B. & Robertson, A.H.F. 1982. Direction of ophiolite emplacement inferred from Cretaceous and Tertiary sediments of an adjacent autochton, the Bey Dağları, southwest Turkey. *Geological Society of America Bulletin* **93**, 68–75.

Hayward, A.B., Robertson, A.H.F. & Scoffin, T. 1996. Miocene patch reefs from a Mediterranean marginal terrigenous setting in southwest Turkey. *In:* Franseen, E.K., Esteban, M., Ward, W.C. & Rouchy, J.-P. (eds), *Models for Carbonate Stratigraphy from Miocene Reef Complexes of Mediterranean Regions.* Society of Economic Mineralogists and Palaeontologists, Concepts in Sedimentology and Palaeontology **5**, 317–332.

Heslop, D. & Dillon, M. 2007. Unmixing magnetic remanence curves without a priori knowledge. *Geophysical Journal International* **170**, 556–566.

Heslop, D., McIntosh, G. & Dekkers, M.J. 2004. Using time- and temperature-dependent Preisach models to investigate the limitations of modelling isothermal remanent magnetization acquisition curves with cumulative log Gaussian functions. *Geophysical Journal International* **157**, 55–63.

Heslop, D., Von Dobeneck, T. & Höcker, M. 2007. Using non-negative matrix factorization in the 'unmixing' of diffuse reflectance spec. *Marine Geology* **241**, 63–78.

Hetzel, R., Passchier, C.W., Ring, U. & Dora, Ö.O. 1995a. Bivergent extension in orogenic belts: the Menderes Massif (southwestern Turkey). *Geology* **23**, 455–458.

Hetzel, R., Ring, U., Akal, C. & Troesch, M. 1995b. Miocene NNE-directed extensional unroofing in the Menderes Massif, southwestern Turkey. *Journal of the Geological Society, London* **152**, 639–564.

Horner, F. & Freeman, R. 1982. Preliminary palaeomagnetic results from the Ionian Zone, western Greece. *EOS* **63**, p. 1273.

Horner, F. & Freeman, R. 1983. Palaeomagnetic evidence from pelagic limestones for clockwise rotation of the Ionian zone, Western Greece. *Tectonophysics* **98**, 11–27.

Hüsing, S.K., Zachariasse, W.J., van Hinsbergen, D.J.J., Krijgsman, W., İnceöz, M., Harzhauser, M., Mandic, O. & Kroh, A. 2009. Oligo–Miocene foreland basin evolution in SE Anatolia: constraints on the closure of the eastern Tethys gateway. *In:* van Hinsbergen, D.J.J., Edwards, M.A. & Govers, R. (eds), *Geodynamics of Collision and Collapse at the Africa-Arabia-Eurasia Subduction Zone.* Geological Society, London, Special Publication **311**, 107–132.

Işık, V., Seyitoğlu, G. & Çemen, İ. 2003. Ductile-brittle transition along the Alaşehir detachment fault and its structural relationship with the Simav detachment fault, Menderes massif, western Turkey. *Tectonophysics* **374**, 1–18.

Jacobshagen, V. 1986. *Geologie von Griechenland*: Berlin-Stuttgart, Borntraeger.

Jolivet, L. 2001. A comparison of geodetic and finite strain pattern in the Aegean, geodynamic implications. *Earth and Planetary Science Letters* **187**, 95–104.

Juteau, T., Nicolas, A., Dubessey, J., Fruchard, J.C. & Bouchez, J.L. 1977. Structural relationships in the Antalya Complex, Turkey: possible model for an oceanic ridge. *Geological Society of America Bulletin* **88**, 1740–1748.

KARABIYIKOĞLU, M., TUZCU, S., ÇİNER, A., DEYNOUX, M., ÖRÇEN, S. & HAKYEMEZ, A. 2005. Facies and environmental setting of the Miocene coral reefs in the late-orogenic fill of the Antalya Basin, western Taurides, Turkey: implications for tectonic control and sea-level changes. *Sedimentary Geology* **173**, 345–371.

KIRSCHVINK, J.L. 1980. The least-squares line and plane and the analysis of palaeomagnetic data. *Geophysical Journal of the Royal Astrological Society* **62**, 699–718.

KISSEL, C., AVERBUCH, O., FRIZON DE LAMOTTE, D., MONOD, O. & ALLERTON, S. 1993. First palaeomagnetic evidence for a post-Eocene clockwise rotation of the Western Taurides thrust belt east of the Isparta reentrant (Southwestern Turkey). *Earth and Planetary Science Letters* **117**, 1–14.

KISSEL, C., JAMET, M. & LAJ, C. 1984. Palaeomagnetic evidence of Miocene and Pliocene rotational deformations of the Aegean Area. *In:* DIXON, J.E. & ROBERTSON, A.H.F. (eds), *The Geological Evolution of the Eastern Mediterranean*. Geological Society, London Special Publications **17**, 669–679.

KISSEL, C. & LAJ, C. 1988. The Tertiary geodynamical evolution of the Aegean arc: a palaeomagnetic reconstruction. *Tectonophysics* **146**, 183–201.

KISSEL, C., LAJ, C. & MÜLLER, C. 1985. Tertiary geodynamical evolution of northwestern Greece: palaeomagnetic results. *Earth and Planetary Science Letters* **72**, 190–204.

KISSEL, C., LAJ, C., POISSON, A. & GÖRÜR, N. 2003. Palaeomagnetic reconstruction of the Cenozoic evolution of the Eastern Mediterranean. *Tectonophysics* **362**, 199–217.

KISSEL, C., LAJ, C., POISSON, A. & SIMEAKIS, K. 1989. A pattern of block rotations in central Aegea. *In:* KISSEL, C. & LAJ, C. (eds), *Palaeomagnetic Rotations and Continental Deformation*, Kluwer Academic Publishers, 115–129.

KISSEL, C. & POISSON, A. 1986. Étude paléomagnetique des formations néogènes du bassin d'Antalya (Taurides occidentales-Turquie). *Comptes Rendus Acadademie Science Paris* **302**, Série II, 711–716.

KISSEL, C. & POISSON, A. 1987. Étude paléomagnetique préliminaire des formations cénozoïques des Bey Daglari (Taurides occidentales, Turquie). *Comptes Rendus Acadademie Science Paris* **304**, Série II, 343–348.

KISSEL, C., SPERANZA, F. & MILICEVIC, V. 1995. Palaeomagnetism of external southern Dinarides and northern Albanides: implications for the Cenozoic activity of the Scutari-Pec shear zone. *Journal of Geophysical Research* **100**, 14999–15007.

KOŞUN, E., POISSON, A., ÇİNER, A., WERNLI, R. & MONOD, O. 2009. Syn-tectonic sedimentary evolution of the Miocene Çatallar Basin, southwestern Turkey. *Journal of Asian Earth Sciences* **34**, 466–479.

KRIJGSMAN, W. & TAUXE, L. 2004. Shallow bias in the mediterranean palaeomagnetic directions caused by inclination error. *Earth and Planetary Science Letters* **222**, 685–695.

KRUIVER, P.P., DEKKERS, M.J. & HESLOP, D. 2001. Quantification of magnetic coercivity components by the analysis of acquisition curves of isothermal remanent magnetisation. *Earth and Planetary Science Letters* **189**, 269–276.

KRUIVER, P.P., LANGEREIS, C.G., DEKKERS, M.J. & KRIJGSMAN, W. 2003. Rock-magnetic properties of multi-component natural remanent magnetisation in alluvial red beds (NE Spain). *Geophysical Journal International* **153**, 317–332.

KRUIVER, P.P. & PASSIER, H.F. 2001. Coercivity analysis of magnetic phases in sapropel S1 related to variations in redox conditions, including an investigation of the S-ratio. *Geochemistry, Geophysics, Geosystems* **2**, 1063, doi:10.1029/2001GC000181.

LAJ, C., JAMET, M., SOREL, D. & VALENTE, J.P. 1982. First palaeomagnetic results from Mio–Pliocene series of the Hellenic sedimentary arc. *Tectonophysics* **86**, 45–67.

LAUER, J.P. 1981. *L'évolution géodynamique de la Turquie et de la Chypre deduite de l'étude palaeomagnetique*. Thesis, Université Strasbourg.

LOURENS, L.J., HILGEN, F.J., LASKAR, J., SHACKLETON, N.J. & WILSON, D. 2004. Chapter 21: The Neogene Period. *In:* GRADSTEIN, F.M., OGG, J.G. & SMITH, A.G. (eds), *A Geologic Time Scale 2004*. Cambridge, Cambridge University Press, 409–440.

MARCOUX, J., RICOU, L.E., BURG, J.-P. & BRUN, J.-P. 1989. Shear-sense criteria in the Antalya and Alanya thrust system (southwestern Turkey): evidence for a southward displacement. *Tectonophysics* **161**, 81–91.

MARTON, E., PAPANIKOLAOU, D.J. & LEKKAS, E. 1990. Palaeomagnetic results from the Pindos, Paxos and Ionian zones of Greece. *Physics of the Earth and Planetary Interiors* **62**, 60–69.

MAURITSCH, H.J., SCHOLGER, R., BUSHATI, S.L. & RAMIZ, H. 1995. Palaeomagnetic results from southern Albania and their significance for the geodynamic evolution of the Dinarides, Albanides and Hellenides. *Tectonophysics* **242**, 5–18.

MAURITSCH, H.J., SCHOLGER, R., BUSHATI, S.L. & XHOMO, A. 1996. Palaeomagnetic investigations in Northern Albania and their significance for the geodynamic evolution of the Adriatic-Aegean realm. *In:* MORRIS, A. & TARLING, D.H. (eds), *Palaeomagnetism and Tectonics of the Mediterranean Region*. Geological Society, London, Special Publications **105**, 265–275.

MCFADDEN, P.L. 1998. The fold test as an analytical tool. *Geophysical Journal International* **135**, 329–338.

MCFADDEN, P.L. & LOWES, F.J. 1981. The discrimination of mean directions drawn from Fisher distributions. *Geophysical Journal of the Royal Astrological Society* **67**, 19–33.

MCFADDEN, P.C. & MCELHINNY, M.W. 1990. Classification of the reversal test in palaeomagnetism. *Geophysical Journal International* **103**, 725–729.

MCFADDEN, P.L., MERRIL, R.T., MCELHINNY, M.W. & LEE, S. 1991. Reversals of the Earth's magnetic field and temporal variations of the dynamo families. *Journal of Geophysical Research* **96**, 3923–3933.

McKenzie, D. 1978. Active tectonics of the Alpine-Himalayan belt: the Aegean Sea and surrounding regions. *Geophysical Journal of the Royal Astrological Society* **55**, 217–254.

Moix, P., Beccaletto, L., Kozur, H.W., Hochard, C., Rosselet, F. & Stampfli, G.M. 2008. A new classification of the Turkish terranes and sutures and its implication for the palaeotectonic history of the region. *Tectonophysics* **451**, 7–39.

Morris, A. 1995. Rotational deformation during Palaeogene thrusting and basin closure in eastern central Greece: palaeomagnetic evidence from Mesozoic carbonates. *Geophysical Journal International* **121**, 827–847.

Morris, A. & Robertson, A.H.F. 1993. Miocene remagnetisation of carbonate platform and Antalya Complex units within the Isparta Angle, SW Turkey. *Tectonophysics* **220**, 243–266.

Mullender, T.A.T., Van Velzen, A.J. & Dekkers, M.J. 1993. Continuous drift correction and separate identification of ferrimagnetic and paramagnetic contribution in thermamagnetic runs. *Geophysical Journal International* **114**, 663–672.

Okay, A.I. 1989. Geology of the Menderes Massif and the Lycian Nappes south of Denizli, western Taurides. *Mineral Research and Exploration (MTA) Bulletin* **109**, 37–51.

Önen, A.P. & Hall, R. 2000. Sub-ophiolite metamorphic rocks from NW Anatolia, Turkey. *Journal of Metamorphic Geology* **18**, 483–495.

Özer, S., Sözbilir, H., Özkar, I., Toker, V. & Sari, B. 2001. Stratigraphy of Upper Cretaceous–Palaeogene sequences in the southern and eastern Menderes Massif (western Turkey). *International Journal of Earth Sciences* **89**, 852–866.

Parlak, O. & Delaloye, M.F. 1999. Precise ^{40}Ar-^{39}Ar ages from the metamorphic sole of the Mersin ophiolite (southern Turkey). *Tectonophysics* **301**, 145–158.

Passier, H.F., de Lange, G.J. & Dekkers, M.J. 2001. Rock-magnetic properties and geochemistry of the active oxidation front and the youngest sapropel in the Mediterranean. *Geophysical Journal International* **145**, 604–614.

Platzman, E.S., Tapirdamaz, C. & Sanver, M. 1998. Neogene anticlockwise rotation of Anatolia (Turkey): preliminary palaeomagnetic and geochronological results. *Tectonophysics* **299**, 175–189.

Poisson, A. 1967. Données nouvelles sur le Crétacé superieur et le Tertiaire du Taurus au NW d'Antalya (Turquie). *Comptes Rendus Academie Science Paris* **264**, 2443–2446.

Poisson, A. 1977. *Récherches géologiques dans les Taurides occidentales (Turquie)*. Thesis, Université de Paris-Sud.

Poisson, A. 1984. The extension of the Ionian trough into southwestern Turkey. *In:* Dixon, J.E. & Robertson, A.H.F. (eds), *The Geological Evolution of the Eastern Mediterranean.* Geological Society, London, Special Publications **17**, 241–250.

Poisson, A., Wernli, R., Sagular, E.K. & Temiz, H. 2003a. New data concerning the age of the Aksu Thrust in the south ofthe Aksu valley, Isparta Angle (SW Turkey): consequences for the Antalya Basin and the Eastern Mediterranean. *Geological Journal* **38**, 311–327.

Poisson, A., Yağmurlu, F., Bozcu, M. & Şentürk, M. 2003b. New insights on the tectonic setting and evolution around the apex of the Isparta Angle (SW Turkey). *Geological Journal* **38**, 257–282.

Price, S.P. & Scott, B.C. 1994. Fault-block rotations at the edge of a zone of continental extension, southwest Turkey. *Journal of Structural Geology* **16**, 381–392.

Reuber, I., Whitechurch, H. & Caron, J.M. 1982. Setting of gabbro dyklets in an ophiolite complex (Antalya, Turkey) by hydraulic fracturing: downward injections of residual liquids. *Nature* **296**, 141–143.

Ricou, L.E., Argyriadis, I. & Marcoux, J. 1975. L'axe calcaire du Taurus, un alignement de fenêtres arabo-africaines sous des nappes radiolaritiques, ophiolitiques et métamorphiques. *Bulletin de la Société Géologique de France* **17**, 1024–1043.

Rimmelé, G., Jolivet, L., Oberhänsli, R. & Goffé, B. 2003. Deformation history of the high-pressure Lycian Nappes and implications for the tectonic evolution of SW Turkey. *Tectonics* **22**, 1007–1029.

Rimmelé, G., Oberhänsli, R., Candan, O., Goffé, B. & Jolivet, L. 2006. The wide distribution of HP-LT rocks in the Lycian Belt (Western Turkey): implications for accretionary wedge geometry. *In:* Robertson, A.H.F. & Mountrakis, D. (eds), *Tectonic Development of the Eastern Mediterranean Region.* Geological Society, London, Special Publications **260**, 447–466.

Robertson, A.H.F. 1993. Mesozoic–Tertiary sedimentary and tectonic evolution of Neotethyan carbonate platforms, margins and small ocean basins in the Antalya Complex, SW Turkey. *In:* Frostick, L.E. & Steel, R. (eds), *Sedimentation, Tectonics and Eustacy: Sea-level Changes at Active Margins*. Special Publication of the International Association of Sedimentologists **20**, 415–465.

Robertson, A.H.F., Poisson, A. & Akinci, Ö. 2003. Developments in research concerning Mesozoic–Tertiary Tetyhs and neotectonics in the Isparta Angle, SW Turkey. *Geological Journal* **38**, 195–234.

Robertson, A.H.F. & Woodcock, N.H. 1980. Strike-slip related sedimentation in the Antalya Complex, S.W. Turkey. *International Association of Sedimentologists Special Publication* **4**, 127–145.

Robertson, A.H.F. & Woodcock, N.H. 1981a. Alakır Çay group, Antalya Complex, SW Turkey: a deformed Mesozoic carbonate margin. *Sedimentary Geology* **30**, 95–131.

Robertson, A.H.F. & Woodcock, N.H. 1981b. Bilelyeri Group, Antalya Complex: deposition on a Mesozoic continental margin in S.W. Turkey. *Sedimentology* **28**, 381–399.

Robertson, A.H.F. & Woodcock, N.H. 1981c. Gödene zone, Antalya Complex: volcanism and sedimentation along a Mesozoic continental margin, S.W. Turkey. *Geologische Rundschau* **70**, 1177–1214.

Robertson, A.H.F. & Woodcock, N.H. 1982. Sedimentary history of the south-western segment of the Mesozoic–Tertiary Antalya continental margin, south-western Turkey. *Eclogae Geologicae Helveticae* **75**, 517–562.

Robertson, A.H.F. & Woodcock, N.H. 1984. The SW. segment of the Antalya Complex, Turkey as a Mesozoic–Tertiary Tethyan continental margin. *In:* Dixon, J.E. & Robertson, A.H.F. (eds), *The Geological Evolution of the Eastern Mediterranean.* Geological Society, London, Special Publications **17**, 251–271.

Sari, B. & Özer, S. 2002. Upper Cretaceous stratigraphy of the Bey Dağları carbonate platform, Korkuteli area (Western Taurides, Turkey). *Turkish Journal of Earth Sciences* **11**, 39–59.

Sari, B., Tasli, K. & Özer, S. 2009. Benthonic foraminiferal biostratigraphy of the upper Cretaceous (middle Cenomanian–Coniacian) sequences of the Bey Dağları carbonate platform, western Taurides, Turkey. *Turkish Journal of Earth Sciences* **18**, 393–425.

Sari, B., Steuber, T. & Özer, S. 2004. First record of Upper Turonian rudists (Mollusca, Hippuritoidea) in the Bey Dağları carbonate platform, Western Taurides (Turkey): taxonomy and strontium isotope stratigraphy of Vaccinites praegiganteus (Toucas, 1904). *Cretaceous Research* **25**, 235–248.

Scheepers, P. 1992. No tectonic rotation for the Apulia-Gargano foreland in the Pleistocene. *Geophysical Research Letters* **19**, 2275–2278.

Şenel, M. 1997. *1/250.000 Scale Geological Maps of Turkey, Fethiye and Antalya Sheets*. Mineral Research and Exploration Institute (MTA) of Turkey Publications.

Şenel, M. 2002. *1/500.000 Scale Geological Map of Turkey, İzmir, Ankara, Denizli and Konya Sheets*. Mineral Research and Exploration Institute (MTA) of Turkey Publications.

Şengör, A.M.C., Görür, N. & Şaroğlu, F. 1985. Strike-slip faulting and related basin formation in zones of tectonic escape: Turkey as a case study. *In:* Biddle, K.T. & Christie-Blick, N. (eds), *Basin Formation and Sedimentation.* Society of Economic Palaeontologists and Mineralogists Special Publications **37**, 227–264.

Şengör, A.M.C. & Yilmaz, Y. 1981. Tethyan evolution of Turkey: a plate tectonic approach. *Tectonophysics* **75**, 181–241.

Speranza, F., Islami, I., Kissel, C. & Hyseni, A. 1995. Palaeomagnetic evidence for Cenozoic clockwise rotation of the external Albanides. *Earth and Planetary Science Letters* **129**, 121–134.

Speranza, F. & Kissel, C. 1993. First palaeomagnetism of Eocene rocks from Gargano: widespread overprint or non-rotation? *Geophysical Research Letters* **20**, 2627–2630.

Speranza, F., Kissel, C., Islami, I., Hyseni, A. & Laj, C. 1992. First palaeomagnetic evidence for rotation of the Ionian zone of Albania. *Geophysical Research Letters* **19**, 697–700.

Spezzaferri, S. 1994. Planktonic foraminiferal biostratigraphy and taxonomy of the Oligocene and Lower Miocene in the oceanic record: an overview. *Palaeontographia Italica* **87**, 1–187.

Stöckli, R., Vermote, E., Saleous, N., Simmon, R. & Herring, D. 2005. The Blue Marble Next Generation – A true color earth dataset including seasonal dynamics from MODIS., http://earthobservatory.nasa.gov/Features/BlueMarble/.

Tauxe, L. & Kent, D.V. 2004. A simplified statistical model for the geomagnetic field and the detection of shallow bias in palaeomagnetic inclinations: was the ancient magnetic field dipolar? *In:* Channell, J.E.T., Kent, D.V., Lowrie, W. & Meert, J.G. (eds), *Timescales of the Palaeomagnetic Field, Geophysical Monograph*. American Geophysical Union **145**, 101–115.

Tauxe, L., Kodama, K.P. & Kent, D.V. 2008. Testing corrections for palaeomagnetic inclination error in sedimentary rocks: A comparative approach. *Physics of the Earth and Planetary Interiors* **169**, 152–165.

Tauxe, L. & Watson, G.S. 1994. The fold test: an eigen analysis approach. *Earth and Planetary Science Letters* **122**, 331–341.

Taymaz, T., Jackson, J. & McKenzie, D. 1991. Active tectonics of the north and central Aegean Sea. *Geophysical Journal International* **106**, 433–490.

Ten Veen, J.H. 2004. Extension of Hellenic forearc shear zones in SW Turkey: the Pliocene–Quaternary deformation of the Esen Çay Basin. *Journal of Geodynamics* **37**, 181–204.

Ten Veen, J.H., Boulton, S.J. & Alçiçek, M.C. 2009. From palaeotectonics to neotectonics in the Neotethys realm: The importance of kinematic decoupling and inherited structural grain inSW Anatolia (Turkey). *Tectonophysics* **473**, 261–281.

Ten Veen, J.H., Woodside, J.M., Zitter, T.A.C., Dumont, J.F., Mascle, J. & Volonskaia, A. 2004. Neotectonic evolution of the Anaximander Mountains at the junction of the Hellenic and Cyprus arcs. *Tectonophysics* **391**, 35–65.

Tirel, C., Gautier, P., van Hinsbergen, D.J.J. & Wortel, M.J.R. 2009. Sequential development of metamorphic core complexes: numerical simulations and comparison to the Cyclades, Greece. *In:* van Hinsbergen, D.J.J., Edwards, M.A. & Govers, R. (eds), *Collision and Collapse at the Africa-Arabia-Eurasia Subduction Zone.* Geological Society, London, Special Publications **311**, 257–292.

Torsvik, T.H., Müller, R.D., Van der Voo, R., Steinberger, B. & Gaina, C. 2008. Global plate motion frames: toward a unified model. *Reviews of Geophysics* **41**, RG3004, doi:10.1029/2007RG000227.

Tozzi, M., Kissel, C., Funiciello, R., Laj, C. & Parotto, M. 1988. A clockwise rotation of southern Apulia? *Geophysical Research Letters* **15**, 681–684.

Uysal, S., Dumont, J.F. & Poisson, A. 1980. *The Platforms of the Western Taurides.* Mineral Research and Exploration Institute (MTA) of Turkey Report no. **6861** [unpublished, in Turkish].

Van Hinsbergen, D.J.J., Dekkers, M.J., Bozkurt, E. & Koopman, M., 2010. Exhumation with a twist: paleomagnetic constraints on the evolution of the Menderes metamorphic core complex (western Turkey). *Tectonics*, **29:** TC2650, doi:10.1029/2009TC 002596.

Van Hinsbergen, D.J.J., Dupont-Nivet, G., Nakov, R., Oud, K. & Panaiotu, C. 2008. No significant post-Eocene rotation of the Moesian Platform and Rhodope (Bulgaria): implications for the kinematic evolution of the Carpathian and Aegean arcs. *Earth and Planetary Science Letters* **273**, 345–358.

Van Hinsbergen, D.J.J., Hafkenscheid, E., Spakman, W., Meulenkamp, J.E. & Wortel, M.J.R. 2005a. Nappe stacking resulting from subduction of oceanic and continental lithosphere below Greece. *Geology* **33**, 325–328.

Van Hinsbergen, D.J.J., Krijgsman, W., Langereis, C.G., Cornée, J.J., Duermeijer, C.E. & van Vugt, N. 2007. Discrete Plio–Pleistocene phases of tilting and counterclockwise rotation in the southeastern Aegean arc (Rhodos, Greece): early Pliocene formation of the south Aegean left-lateral strike-slip system. *Journal of the Geological Society, London* **164**, 1–12.

Van Hinsbergen, D.J.J., Langereis, C.G. & Meulenkamp, J.E. 2005b. Revision of the timing, magnitude and distribution of Neogene rotations in the western Aegean region. *Tectonophysics* **396**, 1–34.

Van Hinsbergen, D.J.J., Zachariasse, W.J., Wortel, M.J.R. & Meulenkamp, J.E. 2005c. Underthrusting and exhumation: a comparison between the External Hellenides and the 'hot' Cycladic and 'cold' South Aegean core complexes (Greece). *Tectonics* **24**, TC2011, doi:10.1029/2004TC001692.

Vandamme, D. 1994. A new method to determine palaeosecular variation. *Physics of The Earth and Planetary Interiors* **85**, 131–142.

Vasiliev I., Franke C., Meeldijk J.D., Dekkers M.J., Langereis C.G. & Krijgsman W. 2008. Putative greigite magnetofossils from the Pliocene epoch, *Nature Geoscience* **1**, 782–786.

Vrielynck, B., Bonneau, M., Danelian, T., Cadet, J.-P. & Poisson, A. 2003. New insights on the Antalya Nappes in the apex of the Isparta Angle: the Isparta Çay unit revisited. *Geological Journal* **38**, 283–293.

Weltje, G.J. 1997. End-member modeling of compositional data: Numerical-statistical algorithms for solving the explicit mixing problem. *Mathematical Geology* **29**, 503–546.

Woodside, J., Mascle, J., Huguen, C. & Volkonskaia, A. 2000. The Rhodes basin, a post-Miocene tectonic trough. *Marine Geology* **165**, 1–12.

Zachariasse, W.J., van Hinsbergen, D.J.J. & Fortuin, A.R. 2008. Mass wasting and uplift on Crete and Karpathos (Greece) during the early Pliocene related to beginning of south Aegean left-lateral, strike slip tectonics. *Geological Society of America Bulletin* **120**, 976–993.

Zijderveld, J.D.A. 1967. A.c. demagnetisation of rocks: analysis of results. *In:* Collinson, D.W. & Al, E. (eds), *Methods in Palaeomagnetism*. Amsterdam, Elsevier, 254–286.

Zitter, T.A.C., Woodside, J.M. & Mascle, J. 2003. The Anaximander Mountains: a clue to the tectonics of southwest Anatolia. *Geological Magazine* **38**, 375–394.